MATERIALS AND METHODS

Site-directed mutagenesis

Site-directed mutagenesis of each Tbx6 binding site was performed using previously reported PCR-based procedures (Yasuhiko et al., 2006) with the following primers (mutated nucleotides in lower case): mB1, 5′-CCTTCGAGGGGTCAGAATCgAtAtCTCTGCAAATGGGCCCGCTTT-3′; mB2, 5′-CCTTCGAGaGtaCtGAATCCACACCTCTGCAAATGG-GCCCGCTTT-3′; mD, 5′-AACCTGGCAGGGGACCACCTCgCgaCTT-TAGTCCAGATAAAAGCT-3′; mG, 5′-CTGGGCTCTGTGGGTTTTG-AattCTCTCTGCAACCTGGCA-3′. The mutated Tbx6 binding sites are indicated for each construct, such that P2EmB1D represents a P2PSME containing both mB1 and mD.

Gene targeting

For targeted disruption of P2PSME, a 356-bp DNA fragment containing mutated Site B and Site D was generated by PCR using primers mB1 and mD. As a negative control, the wild-type P2PSME fragment was also generated by PCR. To construct the targeting vectors, a floxed PGK-neoR selection marker cassette was inserted between a 6-kb long arm and the 356-bp DNA fragment with or without mutations (Fig. 1A). The region corresponding to *Mesp2* exon 1, intron 1 and a part of exon 2 served as the short homology arm. The targeting vector was introduced into mouse ES cells (strain TT2) by electroporation. Resulting G418-resistant ES clones were characterized by PCR using primers: Fesneo, 5′-CGCCTTCT-ATCGCCTTCTTGACGAG-3′ and RP213, 5′-CAGGACAGCCACT-GAGCTGCAGGCCTGA-3′. Southern blots were performed to confirm homologous recombination. Positive ES clones were then aggregated with 8-cell stage ICR mouse embryos in order to produce chimeric mice. The ES selection marker PGK-neoR was removed by crossing the chimeric mice with CAG-Cre mice, which express Cre recombinase ubiquitously. The resulting mouse strains, with insertions of either mutated P2PSME or wild-type P2PSME, were designated P2EmB1D or P2EmCont, respectively. Although the knockout mice were established using an ES cell line (TT2) obtained from a C57BL/6 × CBA cross (Yagi et al., 1993), mice were maintained in an ICR background unless otherwise stated.

Skeletal preparation

Embryonic day 17.5 (E17.5) mouse embryos were obtained by crossing the mutants of interest. Embryos were then fixed with 90% ethanol. For genotyping, PCR was performed using a piece of embryonic liver digested with proteinase K (Roche). Alcian Blue and Alizarin Red staining were performed as described (Saga et al., 1997; Takahashi et al., 2000).

Generation of anti-Tbx6 antibody

His-tagged fragments of Tbx6 protein (N-terminal antigen, amino acids 2-78; internal antigen, amino acids 311-408) (White and Chapman, 2005) were produced using the pET system (Novagen) and *Escherichia coli* Rosetta-gamiB (Novagen) as a host strain. The Tbx6 fragments were extracted from bacterial culture using the MagneHis system (Promega), purified by thrombin digestion to remove the His-tag, followed by affinity column purification (Novagen) and dialysis using a semipermeable membrane cassette (Pierce). Rabbits (two animals for each antigen) were immunized with the purified Tbx6 fragments and processed for antibody purification following the standard procedures of Hokudo Bio (Abuta, Hokkaido, Japan).

Protein and mRNA expression analyses

Whole-mount RNA in situ hybridization was performed as described (Saga et al., 1997). Whole-mount immunohistochemistry and simultaneous staining of *Mesp2* mRNA and Tbx6 protein were as previously described (Morimoto et al., 2005; Oginuma et al., 2008).

Chromatin immunoprecipitation (ChIP) assay

Embryonic tails were dissected along the anteroposterior axis into three parts using a tungsten needle. Somite part (s) corresponds to SIV to SII, anterior PSM (ap) is from SI to S-1, and posterior PSM (pp) corresponds to the region posterior to S-2. A total of 120 embryos were dissected, the samples treated with trypsin and dispersed cells counted (around 1×10^6 cells for each sample). Cells were fixed in 1% formaldehyde in PBS for 10 minutes at 37°C. The preparation of cell lysates and ChIP assay were performed using the Chromatin Immunoprecipitation Assay Kit (Upstate biology) according to the manufacturer's protocol. PCR primers used for ChIP assays were: LP286, 5′-AGACATCCAGGTACCTCGAGGTC-3′; LP287, 5′-CGG-GATAGACATCCAGGTACCCA-3′; and RP287, 5′-GGCTGGTGT-GACTCTGGGAAGCT-3′. LP286 and RP287 were used for detection of mutated P2PSME, whereas LP287 and RP287 were used for detection of wild-type P2PSME. As a positive control, the *Dll1* mesoderm (msd) enhancer was amplified using the following primers: LP259, 5′-CCCAACACAGATGATTCTGCCCAGTAACT-3′; and RP255, 5′-GCT-TTGTGTTGAGCATGCCATGAGCTGTA-3′. A sequence 22 kb from P2PSME was amplified by PCR as a negative control, using the following primers: LP285, 5′-GGTCTGTTTGCAGCTGATTCTGAA-3′; and RP286, 5′-CAGTTCTCACCTTGCTTCCATGT-3′.

Electromobility shift assay (EMSA)

The full-length *Tbx6* ORF was obtained from the pACT-Tbx6 construct, which was previously isolated from a yeast one-hybrid screen (Yasuhiko et al., 2006). After ligation to a 3×FLAG tag (Sigma), the tagged *Tbx6* insert was cloned into pCS2+ (Rupp et al., 1994). In vitro transcription/translation was then performed using the TNT In Vitro Translation Kit (Promega) according to the manufacturer's protocol. Oligonucleotide probes were labeled with DIG-11-ddUTP using recombinant TdT (Roche Diagnostics). Five microliters of crude in vitro translated product was subjected to EMSA. As a negative control, reticulocyte lysate without *Tbx6* template was used. The oligonucleotide probes are as follows (mutated nucleotides are indicated in lower case): SiteF, 5′-GCTAAATTACGGGTATATGGACCACAC-CTGTATCAGTCCC-3′; SiteG, 5′-CTGGGCTCTGTGGGTTTTGACA-CCTCTCTGCAACCTGGCA-3′; SiteGmut, 5′-CTGGGCTCTGTGG-GTTTTGAattCTCTCTGCAACCTGGCA-3′; SiteB, 5′-CCTTCGAGG-GGTCAGAATCCACACCTCTGCAAATGGGCCCGCTTT-3′; T1, 5′-CAAGTGCTGGTCTTGGCATCACACCTCTTTATTTGTTTCCATAC-3′; T2, 5′-GCAGAATCTGCAGAGGTGTCACTTCACACCTCTGTGG-CCTGGCT-3′; and T3, 5′-GCTCTCACAGCTGAGGTGTGAAGCG-ACACCTCCAGGCTCATAAG-3′.

EMSA was performed as described (Yasuhiko et al., 2006). Anti-Tbx6 antibody (3.5 μg) was added to the reaction to assess the specificity of the protein-DNA interaction. As a competitor, a 100-fold excess of unlabeled oligonucleotide corresponding to the probe was added to the reaction.

Transgenic assay

DNA fragments with and without mutations in conserved upstream sites were generated from an *Mesp2* genomic fragment using a standard PCR-based protocol. Each transgene comprised the *lacZ* reporter and a 6-kb genomic fragment upstream of the *Mesp2* first ATG, including P2PSME with and without mutated Tbx6 binding sites. The transgenes were injected into the male pronucleus of a fertilized egg as described (Hogan et al., 1994). Embryos recovered at E9.5-10.5 were analyzed for *lacZ* expression by X-Gal staining (Saga et al., 1992) and were subsequently examined for the presence of the transgene by PCR (Sasaki and Hogan, 1996).

Luciferase assay

The *KpnI-NcoI* fragments (356 bp) corresponding to P2PSME, with and without mutations in the Tbx6 binding sites, were subcloned into the pGL3-Basic (Promega) vector to generate luciferase reporter constructs. The expression vectors for the proteins to be assessed were constructed in the same way as those used in the EMSA assays described above. The luciferase assay using COS-7 cells was conducted as described previously (Yasuhiko et al., 2006). Each assay was performed in triplicate and repeated at least twice.

RESULTS

Mutations in the Tbx6 binding site of the *Mesp2* enhancer result in the complete loss of *Mesp2* expression in the presomitic mesoderm

We have shown previously that nucleotide substitutions in two Tbx6 binding motifs in the *Mesp2* PSM enhancer (P2PSME) eliminate Tbx6 binding activity in vitro (Yasuhiko et al., 2006). To establish the function of these Tbx6 binding sites in vivo, we

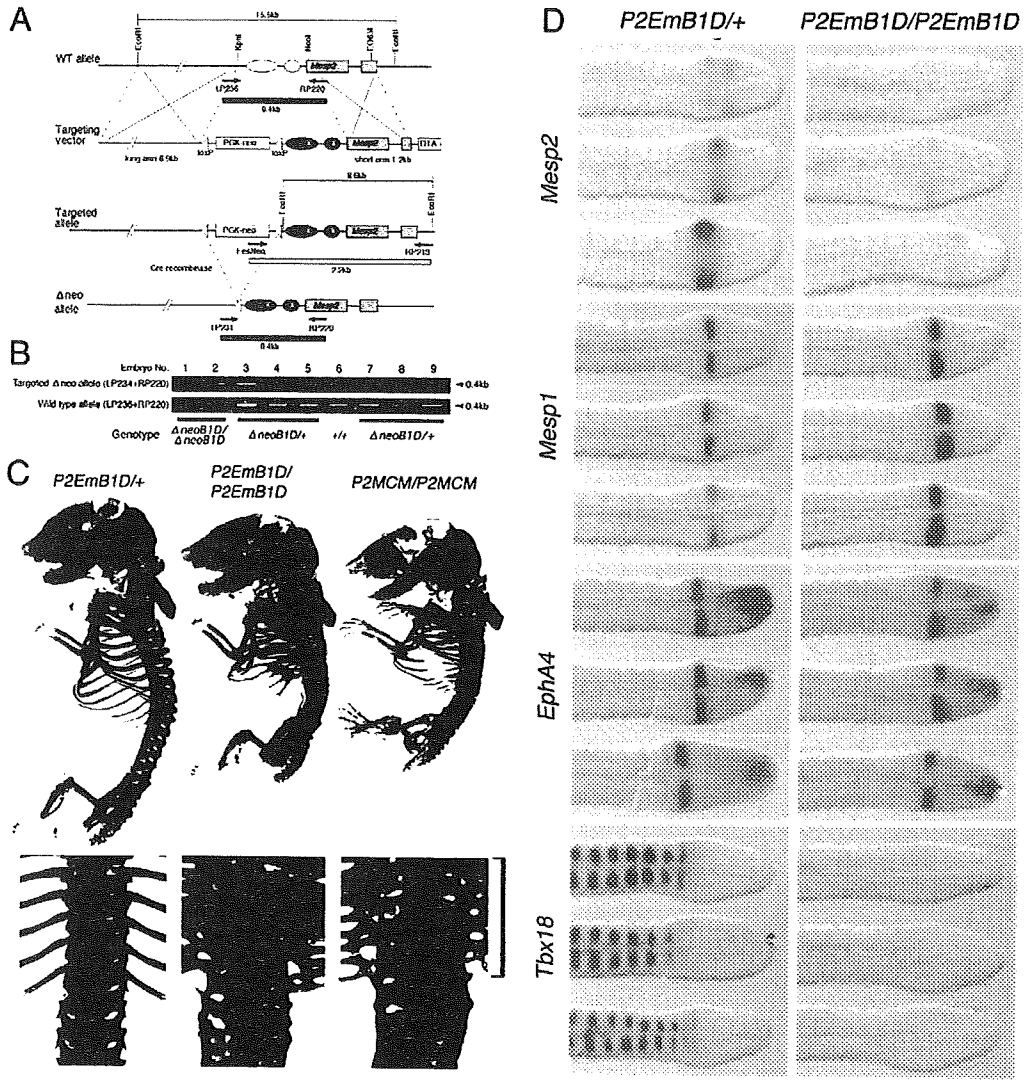

Fig. 1. Disruption of Tbx6 binding sites eliminates *Mesp2* expression. **(A)** Targeting strategy to generate the *Mesp2* enhancer knockout mouse (*P2EmB1D*). A DNA fragment containing mutated Tbx6 binding sites (black ovals with X) was substituted for the wild-type sequence (white ovals) by homologous recombination. The PGK-neoR selection marker was removed by the Cre-loxP system to obtain a Δneo allele. **(B)** PCR detection of homozygotes in the *P2EmB1D* intercross. **(C)** Impaired skeletal segmentation in the *Mesp2* enhancer knockout mouse. The *P2EmB1D/P2EmB1D* mouse exhibits severe skeletal malformation at E17.5 (centre) identical to that of the *Mesp2*-null mouse (*P2MCM/P2MCM*, right). Note the shortened spine with incompletely segmented vertebrae (upper panels) and fused ribs (bracket in lower panels). **(D)** Expression of *Mesp2* and the somite-specific genes *Mesp1*, *Epha4* and *Tbx18* in *P2EmB1D/+* (left column) and *P2EmB1D/P2EmB1D* (right column) embryos. *Mesp2* mRNA expression is eliminated in the *P2EmB1D/P2EmB1D* homozygotes. Wild-type (*+/+*) and heterozygote (*P2EmB1D/+*) embryos showed varying *Mesp2* expression patterns owing to its cyclic expression. *Mesp1* is upregulated and *Epha4* is not affected, whereas *Tbx18* is completely abolished in *P2EmB1D/P2EmB1D*.

introduced nucleotide substitutions into the mouse genome using a gene-targeting technique. These mutations disrupted two Tbx6 binding sites, denoted Site B and Site D, that were shown to be sufficient to activate *Mesp2* expression in vitro (Yasuhiko et al., 2006) (Fig. 1A). After the establishment of a neo*P2EmB1D* mouse line, the neoR cassette was removed (Δneo) by a cross with the deleter mouse line CAG-Cre. Interbreeding of the Δneo mutants gave rise to homozygotes (*P2EmB1D/P2EmB1D*) that retained a loxP site after neoR removal (Fig. 1B). This residual loxP site appears to have no effect on *Mesp2* expression or somitogenesis because another knock-in mouse, *P2EmCont*, in which wild-type P2PSME is knocked-in using the same strategy, had viable homozygous offspring without any morphological defects (data not shown).

The homozygous *P2EmB1D/P2EmB1D* embryos showed distinct skeletal defects (Fig. 1C) and perinatal lethality, features identical to the previously reported Δneo-type *Mesp2*-null mouse (Fig. 1C, *P2MCM/P2MCM*). As expected from the phenotype, *Mesp2* expression in *P2EmB1D/P2EmB1D* embryos was eliminated (Fig. 1D). Segmental borders were generated during an early stage of

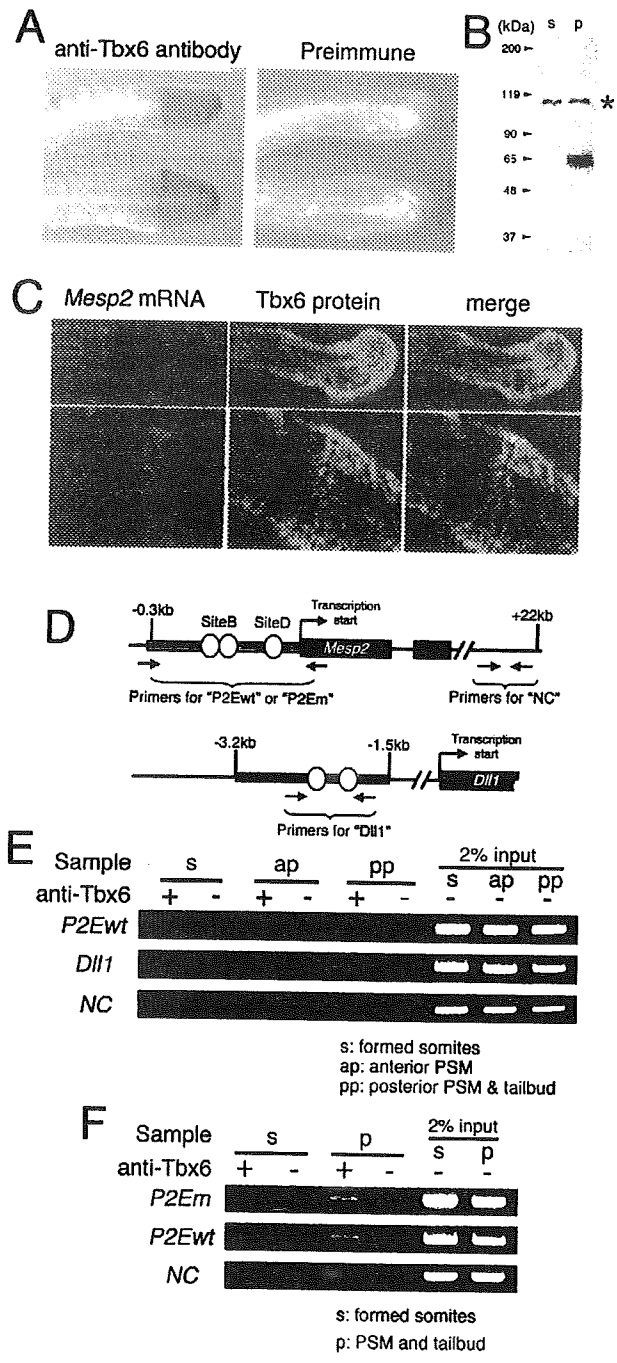

Fig. 2. Tbx6 binds to P2PSME in the PSM and tailbud. (**A**,**B**) Characterization of the anti-Tbx6 antibody produced in this study. (A) Whole-mount immunohistochemistry demonstrating the localization of Tbx6 protein in the mouse PSM and tailbud. (B) Western blot analysis showing that the anti-Tbx6 antibody detected a protein of expected molecular weight (58 kDa) in the PSM and tailbud (p) but not in formed somites (s). The asterisk indicates non-specific binding. (**C**) Double staining of *Mesp2* mRNA (purple) and Tbx6 protein (green) demonstrating the coexistence of both signals in the anterior-most part of the Tbx6-positive region (white in merged image). (**D**) Design of an in vivo technique for detecting Tbx6 binding to the P2PSME by ChIP. Arrows represent primers for the ChIP assay for the *Mesp2* and *Dll1* genes. *Dll1* is known to be downstream of Tbx6 and was therefore used as a positive control. Gray and black boxes represent the P2PSME and *Dll1* mesoderm (msd) enhancers, respectively. White ovals indicate Tbx6 binding sites. P2Em and P2Ewt, mutated and wild-type P2PSME regions, respectively; NC, unrelated sequence as negative control. (**E**) Tbx6 associates with P2PSME in the anterior and posterior PSM. (**F**) The association of Tbx6 with mutated P2PSME as detected by ChIP assay. Mutated and wild-type P2PSME regions were differentially detected by PCR with different sets of primers in the tails of E10.5 embryos obtained from the crossing of *P2EmB1D/+* and ICR mice.

somitogenesis (Fig. 1D, right-hand panels). However, the borders were unlikely to be maintained because the vertebral bodies were fused along the anteroposterior axis at later developmental stages (Fig. 1C).

To further characterize the phenotypes in these embryos, we first examined the expression of *Mesp1*, which is known to be upregulated and to partially rescue somitogenesis in the absence of *Mesp2* (Morimoto et al., 2006; Takahashi et al., 2007). *Mesp1* expression was upregulated in the *P2EmB1D/P2EmB1D* embryo, but its expression domain was broader than normal (Fig. 1D). *Epha4*, which is required for proper border formation, was expressed normally. However, *Tbx18*, which is implicated in the maintenance of segmental border and somite patterning (Bussen et al., 2004), was not expressed (Fig. 1D). These gene expression patterns were similar to those reported for the Δneo-type *Mesp2*-null mouse (Morimoto et al., 2006; Takahashi et al., 2007). These results confirmed that the Tbx6 binding sites are bona fide enhancer elements required for *Mesp2* expression.

Tbx6 binds the *Mesp2* PSM enhancer in vivo

The Tbx6 protein is normally broadly distributed in the PSM and tailbud (White and Chapman, 2005), whereas *Mesp2* is expressed only in the anterior PSM (Saga et al., 1997). This discrepancy between the Tbx6 and *Mesp2* expression patterns prompted us to investigate whether Tbx6 actually binds to the *Mesp2* enhancer in vivo. We raised an anti-Tbx6 antibody using two different antigens: an N-terminal portion of Tbx6 and an internal portion. The internal antigen yielded an antibody with good specificity and sensitivity. Embryo whole-mount immunohistochemistry confirmed the previously reported distinct Tbx6 staining pattern in the PSM and tailbud (Fig. 2A) (White and Chapman, 2005). Western blot analyses further revealed that this antibody identifies a single band of approximately 58 kDa in cell lysates prepared from the posterior region (PSM and tailbud), but not from the anterior region (formed somite), of E11.5 tails (Fig. 2B). We also performed double staining of *Mesp2* mRNA and Tbx6 protein and confirmed colocalization only in the anterior-most region of the PSM (Fig. 2C).

For ChIP assays, we dissected E11.5 embryo tails into three regions: the tailbud and posterior PSM (pp), the anterior PSM and newly formed somites (ap), and formed somites (s). Protein-DNA complexes were prepared from each pool and used in ChIP assays, which revealed that Tbx6 binds to the *Mesp2* PSM enhancer in the ap and pp regions, but not in the s region, which is consistent with the expression pattern of Tbx6 (Fig. 2E). These results indicate that Tbx6 binds to the P2PSME uniformly in its expression domain, suggesting that Tbx6 alone cannot activate *Mesp2* in the posterior PSM where it binds. *Dll1* is known to be a downstream target of Tbx6 and putative binding sites have been identified in its mesoderm

(msd) enhancer (White and Chapman, 2005). ChIP assays using the putative *Dll1* msd enhancer (Fig. 2E, column Dll1) revealed that Tbx6 also binds to the *Dll1* enhancer in both the ap and pp regions, which is consistent with the expression pattern of *Dll1*. In all cases, the negative control (PCR amplification of an unrelated sequence in the mouse genome) gave no signal in ChIP assays with the anti-Tbx6 antibody (Fig. 2E,F, column NC). Thus, these results confirm our previous finding that Tbx6 binding is required for *Mesp2* expression, but is not sufficient for full transcriptional activation.

Mutated P2PSME contains Tbx6 binding sites that are inactive in vivo

We next applied the ChIP assay system to confirm that the phenotype of our enhancer-specific knockout mouse was due to the lack of Tbx6 binding in the *Mesp2* enhancer region. We performed ChIP assays using the tails of *P2EmB1D* heterozygous embryos and specific primer sets in order to distinguish the mutated DNA fragment from its wild-type counterpart, expecting that Tbx6 would not bind to the mutated enhancer. Surprisingly, mutated P2PSME, which has no PSM-specific transcriptional activity (Fig. 1), gave rise to a band that co-precipitated with the anti-Tbx6 antibody. This indicated that Tbx6 still binds to the mutated PSME in vivo (Fig. 2F). To identify the Tbx6 binding site within the mutated P2PSME, we re-examined this region for a consensus Tbx6 binding sequence (White and Chapman, 2005) and found two additional candidate sites, denoted Site F and Site G, in and upstream of P2PSME (Fig. 3A). EMSA demonstrated that Site G was strongly associated with Tbx6 in vitro (Fig. 3B).

The number and spatial organization of the T-box binding sites are important for initiating *Mesp2* transcription via Notch signaling

We reported previously that the simultaneous mutation of two Tbx6 binding sites, Site B and Site D, eliminates PSM-specific activation of a reporter gene by P2PSME in transgenic embryos (Yasuhiko et al., 2006). To confirm this finding and also investigate the possible involvement of the new Tbx6 binding site, Site G, in enhancer activity, we generated a series of reporter constructs with P2PSME harboring serial mutations in the Tbx6 binding sites. We tested two types of reporter assay: a luciferase assay using cultured cells, and transgenic analyses. In the luciferase assay, the loss of any single Tbx6 binding site among Sites B, D and G, caused a 10-fold reduction in Tbx6-dependent and Tbx6 plus Notch signaling-dependent reporter activation (Fig. 3C, right). Conversely, expression of a *lacZ* reporter in transgenic embryos was not markedly affected by the loss of any individual Tbx6 binding site (Fig. 3C, left). These results suggested that each Tbx6 binding site contributes equally to P2PSME activity, but that the loss of a single site is not sufficient to disrupt the in vivo function of P2PSME.

We next examined the effects of systematically removing multiple Tbx6 binding sites. Removal of two Tbx6 binding sites from P2PSME resulted in a further decrease in luciferase reporter activity (Fig. 3C, lane P2EmDG, and Fig. 3D). *lacZ* expression in transgenic embryos was also diminished, both in intensity and frequency. Out of nine transgene-positive embryos, only one showed weak *lacZ* expression with the P2EmB1 reporter, which has two intact Tbx6 binding sites (Fig. 3D, left). When three out of four Tbx6 binding sites were eliminated, the synergistic effects of Tbx6 and Notch signaling on P2PSME activation were no longer observed and mutants resembled P2EmB1DG, which has lost Tbx6 binding capability at all four sites (Fig. 3D, right). In transgenic embryos, *lacZ* expression was not activated by any single Tbx6 binding site (Fig. 3D, left, P2EmB1D). These results strongly suggest that the PSM-specific expression of *Mesp2* requires at least two Tbx6 binding sites in P2PSME. Notably, the P2PSME reporters with two intact Tbx6 binding sites (P2EmDG, P2EmB1, P2EmB2D, P2EmB2G) showed variable levels of activity in the luciferase assay. This finding contrasts with the uniform reporter activity found with either one or three mutated Tbx6 binding sites (Fig. 3C,D). P2EmDG, with two Tbx6 binding sites in Site B intact, displayed a more than 2-fold stronger activity than P2EmB2G, which harbors single Tbx6 binding sites within Site B and Site D. P2EmB2G activated the luciferase reporter at levels comparable to those of reporters with a single Tbx6 binding site and showed no synergistic activation when Notch signaling was applied (Fig. 3D). Taken together, these data indicate that the four Tbx6 binding sites have equal importance in regulating P2PSME activity, and at least two neighboring sites are required for the Notch signaling-dependent induction of *Mesp2* expression.

The medaka *mespb* PSM enhancer regulates *Mesp2* expression and normal somite formation in the mouse embryo

mespb, the zebrafish homolog of *Mesp2*, shows a similar expression pattern to mouse *Mesp2* during embryogenesis and we speculated that it might exert a similar function in the mouse (Nomura-Kitabayashi et al., 2002). We have previously identified the PSM-specific enhancer of medaka *mespb*, which contains T-box binding sites. Two of these sites, T1 and T2, are important for PSM-specific *mespb* expression (Terasaki et al., 2006) (Fig. 4A). These data suggest that the T-box-protein-dependent expression mechanism is evolutionally conserved between mammals and teleosts (zebrafish, medaka). We demonstrated that zebrafish Tbx24, a T-box protein that is homologous to mouse Tbx6 and is responsible for the *fused somite* (*fss*) mutant phenotype, binds to the medaka *mespb* PSME (Fig. 4B). A sequence comparison revealed three putative T-box binding sites in the medaka *mespb* PSME (Fig. 4A). Two of these had the ability to bind two Tbx24 molecules each, whereas in the mouse P2PSME, only Site B can bind two Tbx6 molecules (Fig. 4B).

To more directly demonstrate the evolutionary conservation of this regulatory mechanism, we generated a knock-in mouse with a medaka *mespb* upstream sequence inserted in place of the endogenous *Mesp2* PSME. For this purpose, we substituted the 356-bp sequence upstream of the *Mesp2* first ATG with 2.8 kb of sequence upstream of the *mespb* first ATG, generating a *medakaP2* mouse (Fig. 4C). Heterozygous mice (*medakaP2/+*) were viable and appeared normal (data not shown). Homozygous mice (*medakaP2/medakaP2*) were also viable and showed no physical malformations (Fig. 4D). In skeletal preparations, we observed that *medakaP2* homozygous fetuses were indistinguishable from heterozygous or wild-type littermates (Fig. 4E), indicating that the PSMEs of medaka *mespb* and mouse *Mesp2* are functionally equivalent, despite some differences in their structural features.

DISCUSSION

The activation of *Mesp2* expression requires at least two Tbx6 binding sites in P2PSME

In our current study, we have shown that Tbx6 binding sites are fundamentally important for P2PSME function and that P2PSME is necessary and sufficient for *Mesp2* expression during somite formation in mouse embryogenesis. However, ChIP assays revealed that Tbx6 binds to P2PSME not only in *Mesp2*-expressing cells, but also in non-expressing cells such as those in the tailbud and posterior

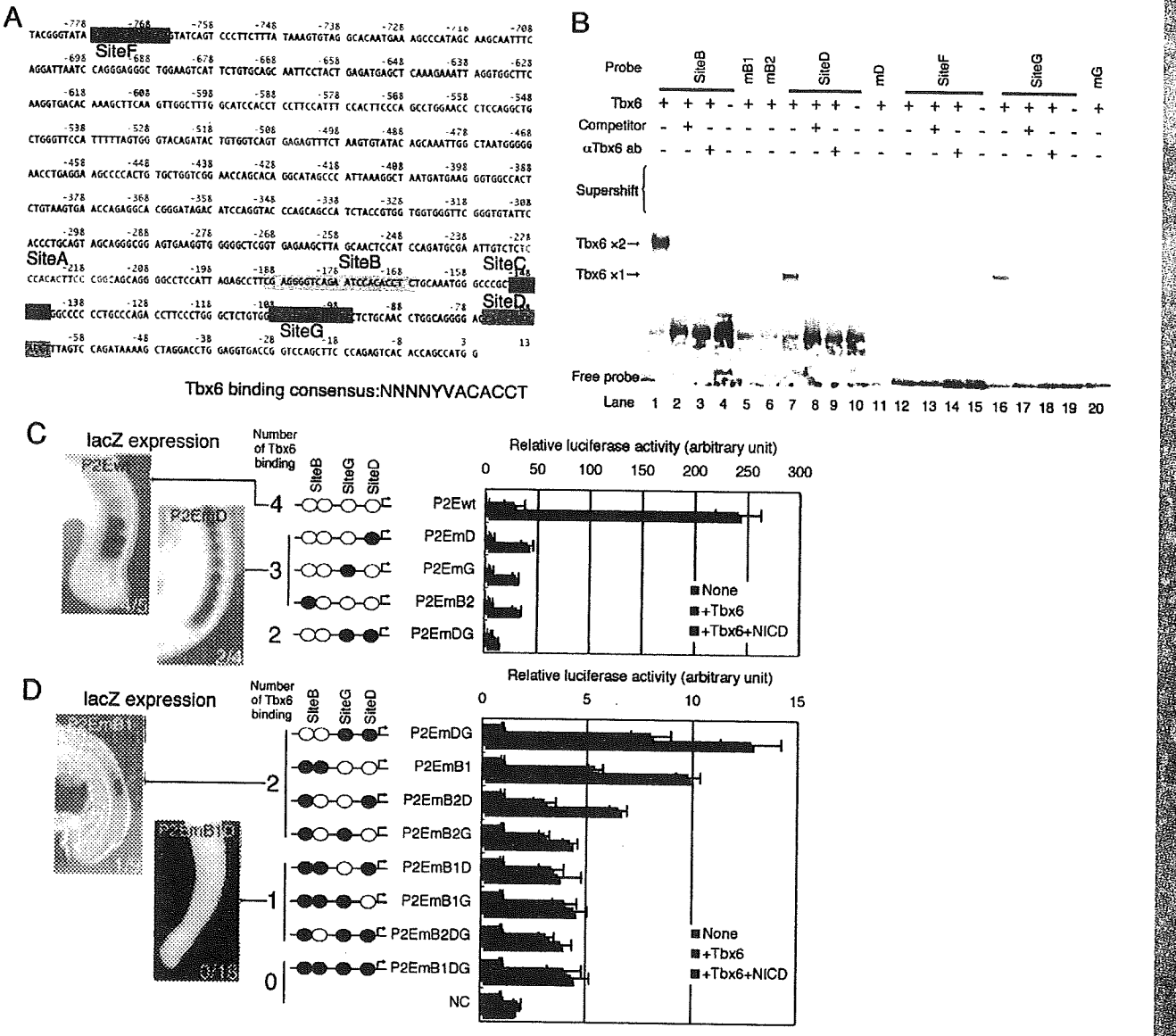

Fig. 3. Multiple Tbx6 binding is required for Mesp2 activation. (**A**) The sequence of the mouse *Mesp2* enhancer region that contains four presumptive Tbx6 binding sites (Sites B, D, F and G). Sites A and C are presumptive RBPJ-κ binding sites (Yasuhiko et al., 2006). The Tbx6 consensus binding site was originally reported by White and Chapman (White and Chapman, 2005). (**B**) Site G, but not Site F, binds to Tbx6 in an electromobility shift assay (EMSA). Site G produced a bandshift indicating a single bound Tbx6 molecule (lane 16), whereas Site B produced two bands (lane 1). Mutated oligonucleotide probes mB1, mD and mG produced no shifted bands (lanes 5, 11 and 20, respectively). The mB2 probe showed a single shifted band, implying the loss of one Tbx6 binding site in Site B (lane 6). (**C**,**D**) Luciferase reporter assays were conducted using several mutated enhancer elements. Luciferase activity was measured after transfection of reporter constructs along with an empty vector (None), Tbx6 expression vector (+Tbx6), or both Tbx6 and Notch intracellular domain expression vectors (+Tbx6 +NICD). Each reporter construct is presented schematically to the left of each graph. Black oval, mutated Tbx6 binding site; white oval, wild-type Tbx6 binding site; arrow, transcription start site. The number of wild-type Tbx6 binding sites is also indicated (number of Tbx6 binding: C, 4 to 2; D, 2 to 0). To the left are representative images of *lacZ* staining in transgenic embryos with P2PSME-*lacZ* reporters bearing the indicated enhancers. The number of *lacZ*-positive/transgene-positive embryos is indicated. The results of a consecutive series of reporter assays, as described in C, are shown in D, but on a different scale owing to the steep declines in activity. The P2EmDG lane represents the same data in both C and D. Each luciferase assay was performed in triplicate in at least three independent experiments. Error bars represent s.d.

PSM (Fig. 2E). This indicates that Tbx6 binding alone is not sufficient to activate *Mesp2* expression. Previously, we showed in vitro that *Mesp2* was activated weakly, if at all, by Tbx6 alone, but rigorously by a coexisting Notch signal (Yasuhiko et al., 2006). Taken together, these data suggest that it is highly likely that the restricted expression pattern of *Mesp2* in the anterior PSM is regulated by a combination of Tbx6 and Notch signaling in vivo. Similarly, Tbx6 activates *Dll1* together with Wnt signaling (Hofmann et al., 2004) and activates *Ripply* in cooperation with Mesp2 (Hitachi et al., 2008). Although the molecular mechanisms

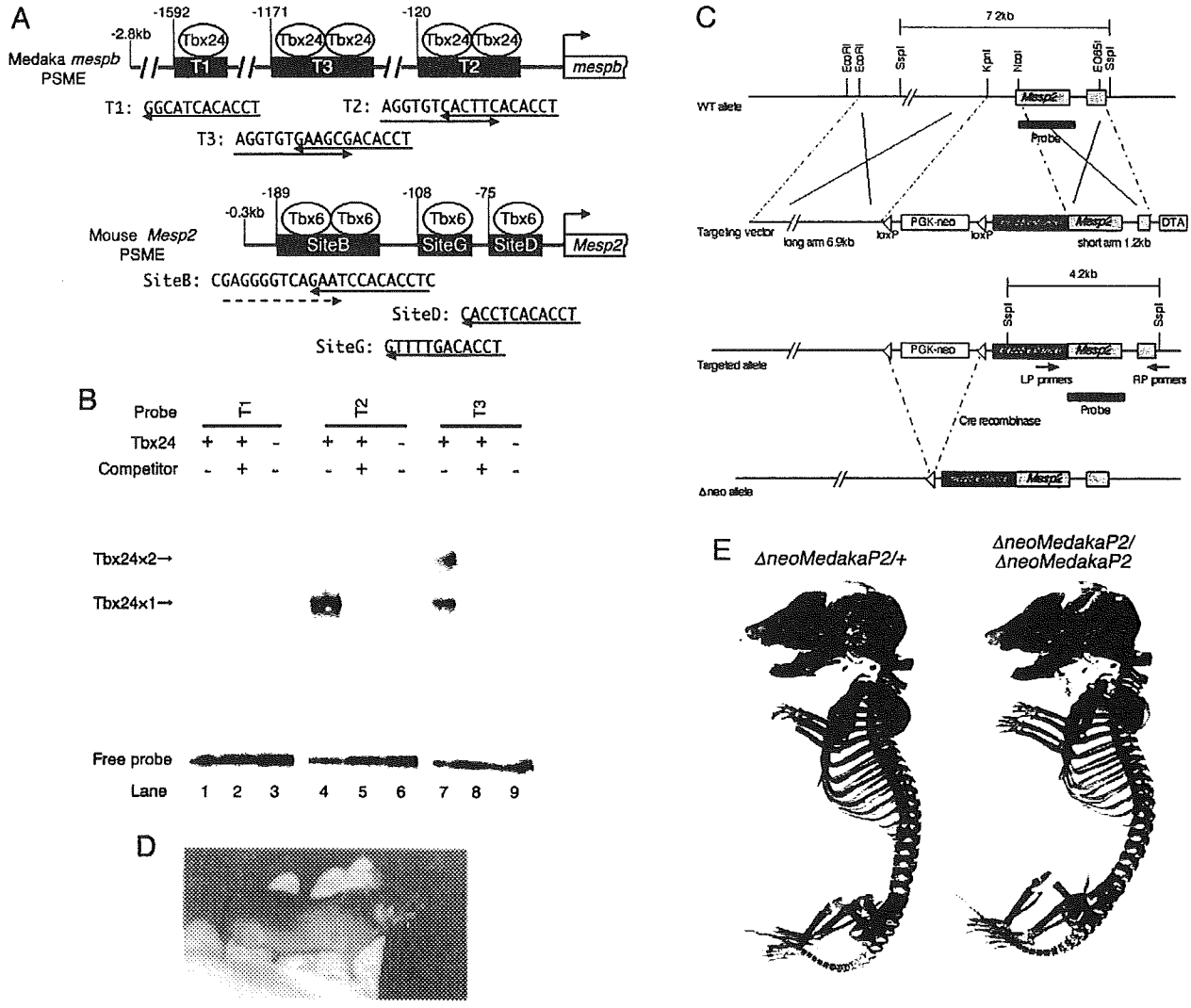

Fig. 4. The medaka *mespb* PSM enhancer is functionally equivalent to its counterpart in the mouse. (**A**) A comparison of the medaka *mespb* and mouse *Mesp2* PSME regions. Black and gray boxes represent presumptive T-box binding sites. The numbers above the boxes represent the nucleotide positions from the first ATG. The nucleotide sequences of the putative T-box binding sequences are shown beneath. Consensus Tbx6 binding sequences and their directions are indicated by arrows. The dashed arrow in Site B of the *Mesp2* PSME depicts an incomplete Tbx6 binding sequence that only binds to Tbx6 if an adjoining complete Tbx6 binding sequence is present. The T-box proteins that might bind to these sequences are indicated. (**B**) EMSA analysis of the T-box binding sites in the medaka *mespb* PSME. T-box binding site T1 associates with a single Tbx24 molecule and T2 and T3 with two Tbx24 molecules, which is consistent with their nucleotide sequences as shown in A. (**C**) The targeting strategy used to generate the medaka *mespb* PSME knock-in mouse (*medakaP2*). A 2.8-kb fragment of *mespb* genomic DNA that is required for PSM-specific *mespb* expression was substituted for *Mesp2* PSME by homologous recombination. The neoR selection marker was removed by recombination using the Cre-loxP system. (**D**) *medakaP2* homozygotes are viable and have normal external features. (**E**) Homozygotes are indistinguishable from heterozygotes and wild-type littermates in skeletal preparations.

by which Tbx6 regulates its target genes together with various partners remain elusive, it is possible that the number and spatial organization of Tbx6 binding sites facilitate the response of P2PSME to Notch signaling.

In total, there are four Tbx6 binding sequences in this region: two palindrome-like sequences in Site B and one each in Sites D and G. Importantly, the P2PSME reporters with only one intact Tbx6 binding site were inactive in both the luciferase assay and the transgenic analyses (Fig. 3D), suggesting that a single P2PSME-bound Tbx6 molecule might not act as a mediator of Notch signaling in the regulatory mechanism controlling *Mesp2* expression. This is consistent with the observation that Site G fails to activate *Mesp2* expression by itself in the *P2EmB1D* mouse.

The loss of two or more of the four Tbx6 binding sites greatly diminishes P2PSME activity in both luciferase and transgenic assays (Fig. 3D). Interestingly, the reporters with two intact Tbx6 binding sites showed varied levels of activity depending upon the position of the intact sites. Two intact Tbx6 binding sites in Site B resulted in the highest reporter activity (Fig. 3D). These data indicate that Site B may be of predominant importance in the function of P2PSME,

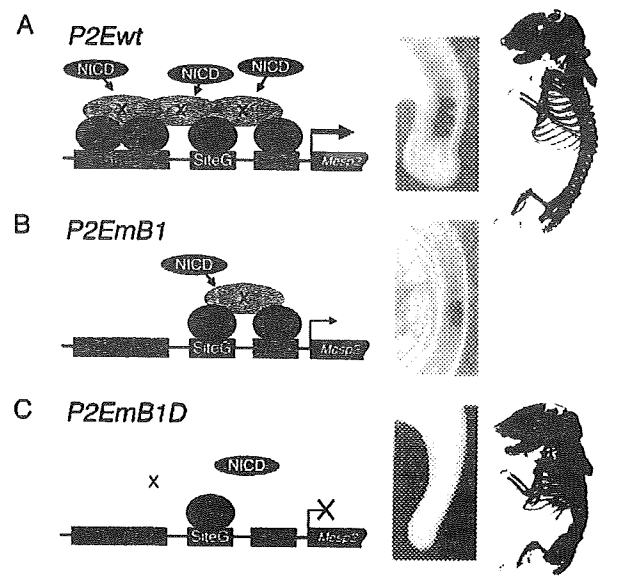

Fig. 5. Putative mechanism for the Tbx6-mediated regulation of Mesp genes. (**A**) Tbx6 activates *Mesp2* expression through multiple Tbx6 binding sites. Notch signaling (NICD, red ovals) activates *Mesp2* expression via factor X (gray ovals), which recognizes two neighboring Tbx6 binding sites in P2PSME. (Left) Schematic description of the Tbx6-dependent activation of *Mesp2*. (Middle column) *lacZ* expression in the P2Ewt transgenic embryo. (Right) Normal skeletal formation in the heterozygous fetus of a *P2EmB1D* mouse. (**B**) Mutation in Site B results in decreased expression of *Mesp2*. (**C**) A single Tbx6 binding site is unable to activate *Mesp2* expression, presumably owing to an inability to respond to Notch signaling.

implying that its two neighboring Tbx6 binding sites play a central role in regulating the activation of *Mesp2*. The binding of Tbx6 to one of the two binding sites in Site B depends on the presence of another Tbx6 molecule binding to this site (Yasuhiko et al., 2006). This property might be related to the unique palindrome-like sequence of this site. Although several T-box binding sites have been identified in the upstream region of other Tbx6-downstream genes, such as *Dll1* (Hofmann et al., 2004) and *Msgn1* (Wittler et al., 2007), the palindrome-like site has thus far been found only in the PSME of *Mesp2* and its medaka ortholog *mespb* (Fig. 4A). It is therefore possible that two neighboring Tbx6 molecules on the palindrome-like site are specifically recognized by as yet unidentified factor(s) (Fig. 5, 'X') that together with Tbx6 constitutes an RBPJ-κ (Rbpj)-independent Notch signaling machinery [disruption of potential RBPJ-κ binding sites does not affect P2PSME activity in transgenic embryos (Yasuhiko et al., 2006)]. Further analyses of *Mesp2* PSME might shed light on these novel regulatory mechanisms that operate during development.

Mutations that removed any one of the Tbx6 binding sites in P2PSME, regardless of which, diminished luciferase reporter activity by the same amount (Fig. 3C), suggesting that each Tbx6 binding site contributes equally to *Mesp2* expression in vitro. In vivo, by contrast, the mutation of a single Tbx6 binding site did not seem to affect PSM-specific gene expression (Fig. 3C). Taken together, these results indicate that the multiple Tbx6 binding sites confer a functional robustness to P2PSME that ensures proper *Mesp2* expression during embryogenesis.

An evolutionally conserved mechanism regulating Mesp expression through multiple T-box binding sites

We previously found that the deletion of two T-box binding sites in the *mespb* PSME greatly reduced its PSM-specific enhancer activity in transgenic medaka embryos (Terasaki et al., 2006), similar to our findings in transgenic mouse embryos. The medaka *mespb* PSME harbors three T-box binding sites (T1-T3), which is similar to the complement of the mouse *Mesp2* PSME (Fig. 4A). However, the total length of the PSME is very different between mouse *Mesp2* and medaka *mespb* (356 bp versus 2.8 kb, respectively) (Terasaki et al., 2006). The number of T-box proteins that bind to the medaka and mouse PSMEs is also different (Fig. 4A,B), and the distance between each element is greater in the *mespb* PSME than in its mouse counterpart.

We have demonstrated, however, that the medaka *mespb* PSME is functionally equivalent to the mouse *Mesp2* PSME. In our transgenic assay, a mutation in the double T-box binding site (Site B in mouse and Site T2 in medaka) had the most profound effect upon PSME activity. Consistent with these results, deletion of medaka Site T1 (harboring a single T-box binding sequence) did not affect reporter gene expression. However, deletion of one of the sites within the double T-box binding sequence (T2) caused a 50% decrease in reporter expression (Terasaki et al., 2006), again demonstrating the importance of the binding to the double T-box site for PSM enhancer function.

In the teleost fish, zebrafish, the T-box transcription factor Tbx24 was identified as responsible for the fused somite (*fss*) mutant phenotype. Tbx24 has a T-box domain that is homologous to that of mouse Tbx6 (Nikaido et al., 2002). The segmentation of somites and expression of *mespb* are eliminated in the *fss* mutant (Sawada et al., 2000), implying that *mespb* is a downstream target of Tbx24, similar to the relationship between *Mesp2* and Tbx6 in mice. However, *fss* mutant fish are viable and fertile (van Eeden et al., 1996), whereas *Tbx6*-null mouse embryos fail to form a mesoderm and die early in development (Chapman and Papaioannou, 1998). This difference might be due to the presence in zebrafish of a *Tbx6* counterpart gene, *spadetail*, which supports paraxial mesoderm formation. Despite this difference, our data clearly demonstrate that the mechanism regulating the PSM-specific expression of *Mesp2* and *mespb* is evolutionarily well conserved between fish and mice.

We thank Hiroyuki Takeda (University of Tokyo) for providing Tbx24 cDNA clones and Mariko Ikumi, Eriko Ikeno and Shunsuke Matsusaka for technical assistance. This work was supported by a grant-in-aid for scientific research from the Ministry of Education, Culture, Sports, Science and Technology, Japan, a grant for Research on Risk on Chemical Substances (H20-004) from the Ministry of Health, Labor and Welfare of Japan, and a grant from the NIG Cooperative Research Program (2007-B66).

References

Bussen, M., Petry, M., Schuster-Gossler, K., Leitges, M., Gossler, A. and Kispert, A. (2004). The T-box transcription factor Tbx18 maintains the separation of anterior and posterior somite compartments. *Genes Dev.* **18**, 1209-1221.

Chapman, D. L. and Papaioannou, V. E. (1998). Three neural tubes in mouse embryos with mutations in the T-box gene Tbx6. *Nature* **391**, 695-697.

Chapman, D. L., Agulnik, I., Hancock, S., Silver, L. M. and Papaioannou, V. E. (1996). Tbx6, a mouse T-Box gene implicated in paraxial mesoderm formation at gastrulation. *Dev. Biol.* **180**, 534-542.

Delfini, M. C., Dubrulle, J., Malapert, P., Chal, J. and Pourquie, O. (2005). Control of the segmentation process by graded MAPK/ERK activation in the chick embryo. *Proc. Natl. Acad. Sci. USA* **102**, 11343-11348.

Dunty, W. C., Jr, Biris, K. K., Chalamalasetty, R. B., Taketo, M. M., Lewandoski, M. and Yamaguchi, T. P. (2008). Wnt3a/β-catenin signaling controls posterior body development by coordinating mesoderm formation and segmentation. *Development* **135**, 85-94.

Galceran, J., Sustmann, C., Hsu, S. C., Folberth, S. and Grosschedl, R. (2004). LEF1-mediated regulation of Delta-like1 links Wnt and Notch signaling in somitogenesis. *Genes Dev.* **18**, 2718-2723.
Haraguchi, S., Kitajima, S., Takagi, A., Takeda, H., Inoue, T. and Saga, Y. (2001). Transcriptional regulation of Mesp1 and Mesp2 genes: differential usage of enhancers during development. *Mech. Dev.* **108**, 59-69.
Hitachi, K., Kondow, A., Danno, H., Inui, M., Uchiyama, H. and Asashima, M. (2008). Tbx6, Thylacine1, and E47 synergistically activate bowline expression in Xenopus somitogenesis. *Dev. Biol.* **313**, 816-828.
Hofmann, M., Schuster-Gossler, K., Watabe-Rudolph, M., Aulehla, A., Herrmann, B. G. and Gossler, A. (2004). WNT signaling, in synergy with T/TBX6, controls Notch signaling by regulating Dll1 expression in the presomitic mesoderm of mouse embryos. *Genes Dev.* **18**, 2712-2717.
Hogan, B., Beddington, R., Costantini, F. and Lacy, E. (1994). *Manipulating the Mouse Embryo: a Laboratory Manual*. Cold Spring Harbor, NY: Cold Spring Harbor Laboratory Press.
Moreno, T. A. and Kintner, C. (2004). Regulation of segmental patterning by retinoic acid signaling during Xenopus somitogenesis. *Dev. Cell* **6**, 205-218.
Morimoto, M., Takahashi, Y., Endo, M. and Saga, Y. (2005). The Mesp2 transcription factor establishes segmental borders by suppressing Notch activity. *Nature* **435**, 354-359.
Morimoto, M., Kiso, M., Sasaki, N. and Saga, Y. (2006). Cooperative Mesp activity is required for normal somitogenesis along the anterior-posterior axis. *Dev. Biol.* **300**, 687-698.
Nikaido, M., Kawakami, A., Sawada, A., Furutani-Seiki, M., Takeda, H. and Araki, K. (2002). Tbx24, encoding a T-box protein, is mutated in the zebrafish somite-segmentation mutant fused somites. *Nat. Genet.* **31**, 195-199.
Nomura-Kitabayashi, A., Takahashi, Y., Kitajima, S., Inoue, T., Takeda, H. and Saga, Y. (2002). Hypomorphic Mesp allele distinguishes establishment of rostrocaudal polarity and segment border formation in somitogenesis. *Development* **129**, 2473-2481.
Oginuma, M., Niwa, Y., Chapman, D. L. and Saga, Y. (2008). Mesp2 and Tbx6 cooperatively create periodic patterns coupled with the clock machinery during mouse somitogenesis. *Development* **35**, 2555-2562.
Rupp, R. A., Snider, L. and Weintraub, H. (1994). Xenopus embryos regulate the nuclear localization of XMyoD. *Genes Dev.* **8**, 1311-1323.
Saga, Y. and Takeda, H. (2001). The making of the somite: molecular events in vertebrate segmentation. *Nat. Rev. Genet.* **2**, 835-845.
Saga, Y., Yagi, T., Ikawa, Y., Sakakura, T. and Aizawa, S. (1992). Mice develop normally without tenascin. *Genes Dev.* **6**, 1821-1831.
Saga, Y., Hata, N., Koseki, H. and Taketo, M. M. (1997). Mesp2: a novel mouse gene expressed in the presegmented mesoderm and essential for segmentation initiation. *Genes Dev.* **11**, 1827-1839.
Sasaki, H. and Hogan, B. L. (1996). Enhancer analysis of the mouse HNF-3 beta gene: regulatory elements for node/notochord and floor plate are independent and consist of multiple sub-elements. *Genes Cells* **1**, 59-72.
Sawada, A., Fritz, A., Jiang, Y. J., Yamamoto, A., Yamasu, K., Kuroiwa, A., Saga, Y. and Takeda, H. (2000). Zebrafish Mesp family genes, mesp-a and mesp-b are segmentally expressed in the presomitic mesoderm, and Mesp-b confers the anterior identity to the developing somites. *Development* **127**, 1691-1702.
Takahashi, Y., Koizumi, K., Takagi, A., Kitajima, S., Inoue, T., Koseki, H. and Saga, Y. (2000). Mesp2 initiates somite segmentation through the Notch signalling pathway. *Nat. Genet.* **25**, 390-396.
Takahashi, Y., Inoue, T., Gossler, A. and Saga, Y. (2003). Feedback loops comprising Dll1, Dll3 and Mesp2, and differential involvement of Psen1 are essential for rostrocaudal patterning of somites. *Development* **130**, 4259-4268.
Takahashi, Y., Yasuhiko, Y., Kitajima, S., Kanno, J. and Saga, Y. (2007). Appropriate suppression of Notch signaling by Mesp factors is essential for stripe pattern formation leading to segment boundary formation. *Dev. Biol.* **304**. 593-603.
Terasaki, H., Murakami, R., Yasuhiko, Y., Shin, I. T., Kohara, Y., Saga, Y. and Takeda, H. (2006). Transgenic analysis of the medaka mesp-b enhancer in somitogenesis. *Dev. Growth Differ.* **48**, 153-168.
van Eeden, F. J., Granato, M., Schach, U., Brand, M., Furutani-Seiki, M., Haffter, P., Hammerschmidt, M., Heisenberg, C. P., Jiang, Y. J., Kane, D. A. et al. (1996). Mutations affecting somite formation and patterning in the zebrafish, Danio rerio. *Development* **123**, 153-164.
White, P. H. and Chapman, D. L. (2005). Dll1 is a downstream target of Tbx6 in the paraxial mesoderm. *Genesis* **42**, 193-202.
Wittler, L., Shin, E. H., Grote, P., Kispert, A., Beckers, A., Gossler, A., Werber, M. and Herrmann, B. G. (2007). Expression of Msgn1 in the presomitic mesoderm is controlled by synergism of WNT signalling and Tbx6. *EMBO Rep.* **8**, 784-789.
Yagi, T., Tokunaga, T., Furuta, Y., Nada, S., Yoshida, M., Tsukada, T., Saga, Y., Takeda, N., Ikawa, Y. and Aizawa, S. (1993). A novel ES cell line, TT2, with high germline-differentiating potency. *Anal. Biochem.* **214**, 70-76.
Yasuhiko, Y., Haraguchi, S., Kitajima, S., Takahashi, Y., Kanno, J. and Saga, Y. (2006). Tbx6-mediated Notch signaling controls somite-specific Mesp2 expression. *Proc. Natl. Acad. Sci. USA* **103**, 3651-3656.

Available online at www.sciencedirect.com
ScienceDirect
Toxicology in Vitro 22 (2008) 1050–1061
Toxicology in Vitro
www.elsevier.com/locate/toxinvit

Screening and detection of the *in vitro* agonistic activity of xenobiotics on the retinoic acid receptor

Ryo Kamata [a,*], Fujio Shiraishi [a], Jun-ichi Nishikawa [b], Junzo Yonemoto [a], Hiroaki Shiraishi [a]

[a] *Research Center for Environmental Risk, National Institute for Environmental Studies, 16-2 Onogawa, Tsukuba, Ibaraki 305-8506, Japan*
[b] *School of Pharmacy and Pharmaceutical Sciences, Mukogawa Women's University, 11-68 Koshien Kubancho, Nishinomiya, Hyogo 663-8179, Japan*

Received 4 October 2007; accepted 4 January 2008
Available online 12 January 2008

Abstract

The retinoic acid receptors (RARs) play key roles in various biological processes in response to endogenous retinoic acids. However, excessive embryonic exposure to specific ligands for each subtype of the RAR was reported to induce specific developmental abnormalities. We measured the RAR agonistic activity of 543 chemicals using an assay system adopting yeast cells transfected with the human RARγ and a coactivator. Eighty-five of the 543 chemicals, including 16 organochlorine pesticides, 14 styrene dimers, 9 monoalkylphenols and 6 parabens, exhibited RARγ agonistic effects in this assay. In particular, monoalkylphenols having a 6–9 carbon alkyl group *para* to the phenolic hydroxyl group possessed high affinity for the RARγ, and their activities were 1.363–0.446% of that of *all-trans* RA. *para*-Alkylphenols chlorinated at the *ortho* position also were about as active or more active than their unchlorinated analogs. In addition, all tested styrene dimers showed positive effects, and the activity of 1-phenyltetralin, the strongest in this category, was 1.169% that of *all-trans* RA. A number of chemicals having binding affinity for the RARγ were revealed in this study (both newly identified and confirmed), further comprehensive studies of *in vitro* and *in vivo* effects via the RARs are required for the reliable risk assessment of chemicals. *In vitro* receptor binding studies represent an important step in hazard identification and suggest a potential mechanism of action, which can be an important step in risk assessment and in particular for screening studies to identify potential toxicity and inform mechanistic studies.

Keywords: Retinoic acid receptor; Two-hybrid yeast assay; Monoalkylphenol; Styrene dimer; Paraben; Organochlorine pesticide

1. Introduction

The retinoic acid (RA) receptors (RARs) are, like the steroid hormone and thyroid hormone receptors (TR), nuclear receptors that respond to specific natural ligands, *all-trans* RA and 9-*cis* RA. Both RAs, which are oxidative metabolites of vitamin A, are essential for cellular proliferation, development and differentiation in vertebrates and therefore play crucial roles in normal growth and homeostasis. However, both deficiency and excess of vitamin A are harmful. Vitamin A deficiency during gestation results in diverse embryonic malformations in various organs (Zile, 1998, 2001), while excess RA has been reported to trigger teratogenic actions in the developing embryo via the RARs. Ligands specific for each subtype of the RARs (α, β and γ) have been reported to induce specific deformities in rodent embryos (Elmazar et al., 1996, 2001). A ligand for the α-subtype causes defects of the ear, mandible and limb, a β-subtype ligand causes defects of the urinary system and liver, and a γ-subtype ligand causes ossification deficiencies and defects of the sternebrae and vertebral body.

We have developed several yeast two-hybrid systems transduced with the ligand binding domains of nuclear receptors and a coactivator for the receptors for detecting and measuring the activity of chemicals (Nishikawa et al., 1999; Shiraishi et al., 2000). In prior works, it has been found that there are a number of industrial/environmental compounds with the capability to activate or inactivate nuclear receptors such as the estrogen receptors (ERs)

* Corresponding author. Tel.: +81 29 8502873; fax: +81 29 8502870.
E-mail address: kamata.ryo@nies.go.jp (R. Kamata).

0887-2333/$ - see front matter © 2008 Elsevier Ltd. All rights reserved.
doi:10.1016/j.tiv.2008.01.002

and the TRs, and some compounds show unexpected activity; i.e., activity that would not be readily predicted from the structure of the compounds (Shiraishi et al., 2003; Arulmozhiraja et al., 2005; Morohoshi et al., 2005). These studies indicated that chemicals encountered in daily life or through accidental exposure bind with nuclear receptors and suggested potential toxicity, mechanisms of action and therefore potential risks to human health. In our laboratory, yeast assays with nuclear receptors derived from the Japanese medaka fish (*Oryzias latipes*) as well as the human have also demonstrated the receptor activation of environmental water samples taken from contaminated rivers, lakes and seas (Mispagel et al., 2005; unpublished data, Shiraishi et al., 2006) and thereby show that organisms in the environment may be exposed to potentially harmful chemicals and/or bioactive substances originating from human activity.

The objective of the present study was to screen a wide range of xenobiotic and other compounds for agonistic effects on the RAR and to quantify their activities. We prepared a yeast two-hybrid system to detect transcriptional activation via the human RARγ and assessed 543 compounds including industrial chemicals, agrochemicals, natural compounds, medicines and cosmetic chemicals. An assay for each human RAR subtype was derived from previously reported yeast assays and optimized for high-throughput screening. Because the yeast cells transfected with the γ-subtype showed the lowest luminescence intensity when inactivated and the highest reactivity to an endogenous ligand, *all-trans* RA, we selected the RARγ type of assay for the present investigation. As the RAR agonistic effect was detected in different categories of chemicals, we provide the measured activities of the positively-reacting compounds grouped according to chemical structure.

2. Materials and methods

2.1. Compounds

The 543 compounds examined in this study are listed in Table 1, grouped according to their intended uses and chemical structures. The compounds were purchased from Accu Standard, Inc. (New Haven, CT, USA), Acros Organics N.V. (Geel, Belgium), Alfa Aesar GmbH & Co., KG (Karlsruhe, Germany), Cosmo Bio Co., Ltd. (Tokyo, Japan), Dr. Ehrenstorfer GmbH (Augsburg, Germany), GL Science, Inc. (Tokyo, Japan), Hayashi Pure Chemical Industries, Ltd. (Osaka, Japan), Kanto Chemical Co., Inc. (Tokyo, Japan), Katayama Chemical Industries Co., Ltd. (Osaka Japan), Nacalai Tesque, Inc. (Kyoto, Japan), Maruzen Petrochemical Co., Ltd. (Tokyo, Japan), MP Biochemicals (Solon, OH, USA), PerkinElmer, Inc. (Wellesley, MA, USA), Scientific Polymer Products, Inc. (Ontario, NY, USA), Sigma–Aldrich Corp. (St. Louis, MO, USA), Steraloids, Inc. (Newport, RI, USA), Tocris Bioscience (Ellisville, MO, USA), Tokyo Chemical Industry Co., Ltd. (Tokyo, Japan), Toronto Research Chemicals Inc. (North York, ON, Canada) and Wako Pure Chemical Industries, Ltd. (Osaka, Japan), or were gifts from researchers who had synthesized them for other purposes.

2.2. Yeast two-hybrid assay

The transcriptional agonistic activities of compounds to the RAR were measured with a reporter assay using yeast cells (*Saccharomyces cervisiae* Y190). An expression plasmid for the ligand binding domain of the human RARγ and the coactivator pGAAD424-TIF-2 was introduced into yeast cells that carried the β-galactosidase reporter gene (Nishikawa et al., 1999). The assay was performed using a chemiluminescent reporter gene method (for β-galactosidase) employing a 96-well culture plate, based on a yeast two-hybrid estrogenicity assay (Shiraishi et al., 2000, 2003).

Yeast cells were preincubated for 24 h at 30 °C with shaking in modified SD medium lacking tryptophan and leucine (5.8% yeast nitrogen base, 0.75% dextrose, 0.013% L-valine, 0.00435% L-phenylalanine, 0.00261% L-isoleucine, L-lysine HCl and L-tyrosine, 0.00174% L-adenine hemisulfate salt, L-arginine HCl, L-histidine HCl monohydrate, L-methionine and L-uracil) and the cell density was adjusted to an absorbance of 1.65–1.80 at 595 nm. A dimethylsulfoxide (DMSO) solution of each test compound was stored at −80 °C until just before examination and was serially twofold diluted with the medium. An aliquot of the diluted solution (120 μl) was poured to two wells of a black 96-well culture plate for chemiluminescence measurement, and then the yeast cell suspension (60 μl) was added. At least seven serial two-fold concentrations of each chemical from 10 μM to 156 nM were tested; lower concentrations were tested for chemicals showing high RAR agonistic activity. The solution in every well contained 1% DMSO. After vortex mixing, the plate was incubated at 30 °C under conditions of high humidity for 4 h. A solution (80 μl) for inducing chemiluminescence from released β-galactosidase, consisting of reaction buffer (30 μl) containing GalactLux substrate (AURORA GAL-XE, MP Biochemicals) and a 1:1 mixture (50 μl) of zymolyase 20 T and 100 T solutions for enzymatic digestion (Kirin Brewery Co, Ltd., Tokyo, Japan), was added to each well. The plate was incubated at 37 °C for 1 h and then placed in a 96-well plate luminometer (Luminescencer-JNR AB-2100, ATTO, Tokyo, Japan), and a light emission accelerator solution (AURORA GAL-XE, 50 μl) was added to each well using the luminometer pump. The chemiluminescence produced by released β-galactosidase in each well was measured.

All test compounds were evaluated in a minimum of three separate assays which were performed in duplicate. For comparative estimates of the ability of test compounds to activate the RAR, *all-trans* RA, an endogenous agonist of RAR, was used as a standard. A DMSO solution of *all-trans* RA was stored in a shielding container at −80 °C until just before examination to prevent degradation, and seven serial twofold concentrations of *all-trans* RA were examined for every culture of yeast cells. A dose-response

Table 1
List of 543 compounds tested in a yeast two-hybrid assay for the RARγ

Compounds
Industrial chemicals (252)
Aromatic hydrocarbons (10)
Biphenyl
2-Terphenyl
3-Terphenyl
4-Terphenyl
n-Butylbenzene
n-Octylbenzene
n-Nonylbenzene
1,3-Diphenylpropane
Benzylbiphenyl
Triphenylmethane
Polycyclic aromatic hydrocarbons (14)
Naphthalene
Acenaphthene
Fluorene
Phenanthrene
Anthracene
Pyrene
Fluoranthene
Chrysene
Benz[a]anthracene
Benzo[a]pyrene
Benzo[e]pyrene
Benzo(k)fluoranthene
Benzo(b)fluoranthene
Dibenz(a,h)anthracene
Arsenic compounds (13)
Sodium meta-arsenite
Dimethyl arsinic acid
Methyl arsonic acid
Arsenic(III)oxide
Phenyldimethylarsine oxide
Phenylmethylarisine oxide
Phenyl arsonic acid
Diphenylmethylarsine oxide
Diphenyl arsinic acid
Triphenyl arsine
Sodium arsenate (dibasic) 7H2O
Triphenyl arsine oxide
10,10'-Oxybis(phenoxyarsine)
Bisphenols and related chemicals (37)
Octafluoro-4,4'-biphenol
2,2',6,6'-Tetramethylbisphenol A
4,4'-Thiodiphenol
Bisphenol A
2,2',6,6'-Tetrabromobisphenol A
2,2',6,6'-Tetrachlorobisphenol A
Bisphenol B
2-Chlorobisphenol A
2,2'-Dichlorobisphenol A
2,6-Dichlorobisphenol A
2,2',6-Trichlorobisphenol A
4,4'-Methylenebisphenol (Bisphenol F)
4,4'-Sulfonyldiphenol (Bisphenol S)
3,4-(1-Methyl-1-phenylethyl)diphenol
2,4'-Isopropylidenediphenol
4,4'-(1,3-Dimethylbutylidene)bisphenol
Bisphenol E
2,4'-Dihydroxydiphenyl sulfone (Bisphenol S iso.)
2,2'-Isopropylidenediphenol
4,4'-Cyclohexyliden bisphenol
4,4'-(1-Ethyl-2-methyltrimethylene)bisphenol
4,4'-Diisobutylethylidenediphenol
4-Hydroxyacetophenone
4-Hydroxy-4'-isopropoxy diphenylsulfone
4,4'-Isopropoxy diphenylsulfone
4-[1-(4-Hydroxyphenyl)-1-methylethyl]-1,2-benzoquinone
Bisphenols and related chemicals (Continued)
4-Hydroxyphenyl isopropanol
4-Hydroxyphenyl isobutyl methyl ketone
6-Hydroxy-1-(4-hydroxyphenyl)-1,3,3-trimethylindane
4-Cumylphenol
2-(4-Hydroxyphenyl)-2,4,4-trimethylchroman
6-Hydroxy-3-(4-hydroxyphenyl)-1,1,3-trimethylindane
2,4-Bis(4-hydroxycumyl)phenol
4-(4-Hydroxyphenyl)-2,2,4-trimethylchroman
4-Propenylphenol
4-Methyl-2,4-bis(p-hydroxyphenyl)pent-1-ene
2-(2-Hydroxyphenyl)-2,4,4-trimethylchroman
Dyes (21)
Azobenzene
N-Acetyl-5-hydroxy-tryptamine
Acid Alizarin Violet N
1-Acetyl-4-(4-hydroxyphenyl)-piperazine
Anthrarobin
Anthraflavic acid
cis-1,3-O-Benzylideneglycerol
Chlorophenol Red
2,5-Dihydroxyphenylacetic γ-lactone
4-(2,4-Dinitroanilino)-phenol
6-Fluoro-4-hydroxy-coumarin
Hoechst 33258
6-Hydroxy-1,3-benzoxathiol-2-one
2-Hydroxy-9-fluorenone
4-Hydroxyindole
4-Hydroxy-6-methyl-2-pyrone
3-Hydroxy-1H-phenalen-1-one
2-(4-Hydroxyphenyl)-5-pyrimidinol
1-Hydroxypyrene
Indigo. carmine
Indigo, synthetic
Metals (5)
Tributyltin(IV)chloride
Triphenyltin(IV)chloride
Dibutyltin(IV)dichloride
Lead (II) chloride
Lead (II) acetate trihydrate
Monoalkyl phenols and related chemicals (27)
2-n-Propylphenol
3-n-Propylphenol
4-n-Propylphenol
2-Isopropylphenol
3-Isopropylphenol
4-Isopropylphenol
4-n-Butylphenol
2-s-Butylphenol
4-s-Butylphenol
2-t-Butylphenol
3-t-Butylphenol
4-t-Butylphenol
4-n-Pentylphenol
4-t-Pentylphenol
4-n-Hexylphenol
4-n-Heptylphenol
4-n-Octylphenol
4-t-Octylphenol
4-n-Nonylphenol
4-Nonylphenol (mixed isomers)
4-Dodecylphenol (mixed isomers)
2-Chloro-4-butylphenol
2,6-Dichloro-4-butylphenol
2-Chloro-4-octylphenol
2,6-Dichloro-4-octylphenol
2-Chloro-4-nonylphenol
2,6-Dichloro-4-nonylphenol
Parabens (13)
3-Hydroxybenzoic acid
4-Hydroxybenzoic acid
Methyl 4-hydroxybenzoate
Ethyl 4-hydroxybenzoate
Propyl 4-hydroxybenzoate
Isopropyl 4-hydroxybenzoate
Butyl 4-hydroxybenzoate
Isobutyl 4-hydroxybenzoate
n-Amyl 4-hydroxybenzoate
n-Hexyl 4-hydroxybenzoate
Benzyl 4-hydroxybenzoate
2-Ethylhexyl 4-hydroxybenzoate
n-Dodecyl 4-hydroxybenzoate
Phenols and related chemicals (37)
4-Cyanophenol
4-Hydroxybenzaldehyde
4-Methoxyphenol
2-Cyclopentylphenol
4-Cyclopentylphenol
2,4-Dichlorophenol
3,4-Dichlorophenol
4-Hydroxycinnamic acid
2-Hydroxybiphenyl
4-Hydroxybiphenyl
4-Cyclohexylphenol
4-Benzylphenol
4-Hydroxybezophenone
Phenyl salicylate
2-Iodophenol
4-Iodophenol
1,1-Bis(4-hydroxyphenyl)-propane
4-(1-Adamantyl)phenol
2-(1-Adamantyl)-4-methylphenol
2,4-Dibromophenol
2,6-Dibromophenol
3-(4-Hydroxyphenyl)propionic acid N-hydroxysuccinimide ester
Hexestrol
4,4-Bis-(4-hydroxyphenyl)valeric acid
Phenolphthalein
4,4'-(1,3-Adamantane-diyl)diphenol
2,4,6-Tribromophenol
3,5-Diiodosalicylic acid
Butylphenoxy acetic acid
2,3-Dichlorophenoxy acetic acid
2-Chloro-4-butylphenoxy acetic acid
4-Nonylphenyl 2-hydroxyethyl ether
2,6-Dichloro-4-butylphenoxy acetic acid
2-Chloro-4-nonylphenyl 2-hydroxyethyl ether
2-Chloro-4-octylphenoxy acetic acid
4-Nonylphenyl 2-(2hydroxy-ethyloxy)ethyl ether
2,6-Dichloro-4-nonylphenyl 2-hydroxyethyl ether
Phthalates (9)
Diethyl phthalate
Di-n-propyl phthalate
Di-n-butyl phthalate
Di-n-pentyl phthalate
Benzyl n-butyl phthalate
Dicyclohexyl phthalate
Di-n-hexyl phthalate
Dibenzyl terephthalate
Di-2-ethylhexyl phthalate

Table 1 (*continued*)

Compounds		
Industrial chemicals (Continued)	Agrochemicals (124)	Organophosphates (Continued)
Styrene dimers (14+1)	Amides (2)	EPN
1,4-Diphenyl-2-butene	Mepronil	Ethion
1-Methyl-1-phenylindan	Flutolanil	Glyphosate
1-Methyl-3-phenylindan		Iprobenfos
1-Phenyltetralin	Benzimidazoles (2)	Isofenphos
2,3-Diphenyl-1-butene	Carbendazim	Isofenphos oxon
2,4-Diphenyl-1-butene	Thiabendazole	Isoxathion
cis-1,4-Diphenyl-1-butene		Isoxathion oxon
trans-1,4-Diphenyl-1-butene	Carbamates (12)	Leptophos
cis-2,4-Diphenyl-2-butene	Aldicarb	Malathion
trans-2,4-Diphenyl-2-butene	Benfuracarb	MEP oxon
cis-1,2-Diphenylcyclobutane	Benomyl	Parathion
trans-1,2-Diphenylcyclobutane	Carbaryl (NAC)	Phenthoate
trans-1,3-Diphenyl-1-butene	Mancozeb	Piperophos
trans-1,3-Diphenylcyclobutane	Maneb	Prothiophos
Polystyrene standard (mixed styrene dimer isomers)	Methomyl	Thenylchlor
	Metiram	Tolclofos-methyl
Styrene trimer (16)	Molinate	
1,2,4-Triphenylcyclohexane	Thiobencarb	Pyrethroids (16)
1,3,5-Triphenyl-1-hexene	Zineb	Allethrin
1,3,5-Triphenylcyclohexane	Ziram	cis-Permethrin
1,4,5-Triphenyl-1-hexene		Cycloprothrin
1a-Phenyl-4a-(1-phenylethyl)-1,2,3,4-tetrahydronaphthanene	Diphenyl ethers (7)	Cyfluthrin
1a-Phenyl-4a-(2-phenylethyl)tetralin	Acifluorfen	Cyhalothrin
1a-Phenyl-4e-(1-phenylethyl)-1,2,3,4-tetrahydronaphthanene	Aclonifen	Cypermethrin
1e,2e,4a-Triphenylcyclohexane	Bifenox	Esfenvalerate
1e-Phenyl-4a-(1-phenylethyl)-1,2,3,4-tetrahydronaphthanene	Chlomethoxynil	Ethofenprox
1e-Phenyl-4a-(2-phenylethyl)tetralin	Chlornitrofen (CNP)	Fenpropathrin
1e-Phenyl-4e-(1-phenylethyl)-1,2,3,4-tetrahydronaphthanene	CNP-amino	Fenvalerate
1-Methyl-1,2,4-triphenylcyclopentane	Nitrofen	Flucythrinate
1-Methyl-1,3,4-triphenylcyclopentane		Fluvalinate
1-Methyl-3-phenyl-2-(1-phenylethyl)indan	Organochlorines (30)	Permethrin
2,4,6-Triphenyl-1-hexene	Aldrin	Resmethrin
2,4,6-Triphenyl-2-hexene	β-Benzene hexachloride (β-BHC)	Tralomethrin
	Chlordane	trans-Permethrin
Others (35)	cis-Chlordane	
4-Nitrotoluene	trans-Chlordane	Triazines (4)
1-Naphthol	Chlordecone	Atrazine
2-Naphthol	o,p'-DDD	Dimethametryn
4-Hydroxy-1-indanone	o,p'-DDE	Metribuzin
5,6,7,8-Tetrahydro-1-naphthol	o,p'-DDT	Simazine (CAT)
5,6,7,8-Tetrahydro-2-naphthol	p,p'-DDD	
Sodium pyrithione	p,p'-DDE	Ureas (2)
1,2-Benzothiazol-3-one	p,p'-DDT	Diuron
Biphenyl ether	Dicofol	Pencycuron
2-n-Octyl-4-isothiazolin-3-one	Dieldrin	
N,N',N''-Trishydroxyethylhexahydro-s-triazine	α-Endosulfan	Others (22)
Benzyl-2-naphthylether	β-Endosulfan	Alachlor
4-Nonylcatechol	Endrin	Amitrole
1-(4-Hydroxyphenyl)-1-nonanol	Fthalide	Bromofenoxim
Methyl o-benzoylbenzoate	Heptachlor	Buprofezin
1,2-Bis(3-methylphenoxy)ethane	cis-Heptachlor epoxide	Captan
Triphenylborane	trans-Heptachlor epoxide	Chlorotharonil
1-Nitropyrene	Hexachlorobenzene	Coumachlor
2-Iodobenzoic Acid	1,2,3,4,5,6-Hexachlorocyclohexane (γ-BHC)	Dazomet
Dipyrithione	Methoxychlor	1,2-Dibromo-3-chloropropane (DBCP)
6-Bromoharman	Mirex	Dichlofluanid
Phenyl-1-hydroxy-2-naphthoate	trans-Nonachlor	(2,4-Dichlorophenoxy)acetic acid
β-Naphthoflavone	Oxychlordane	2-(3-Chlorophenoxy)-propionic Acid
Zinc pyrithione	Pentachlorophenol (PCP)	1,3-Dichloropropene
Triphenylborane-pyridine complex	Toxaphene	Fluazifop-butyl
6,8-Dibromoharman	2,4,5-Trichlorophenoxyacetic Acid	Oxadiazon
meso-Stilbene dibromide		Pendimethalin
Copper quinolate	Organophosphates (27)	Probenazole
Di(2-ethylhexyl)adipate	Bromophos-ethyl	Pyroquilon
Octachlorostyrene	Bromopropylate	Tebuconazole
3,6,8-Tribromoharman	Butamifos	Tebufenozide
Triphenylborane-octadecylamin complex	Chlorpyrifos	Trifluralin
Perfluorobutansulfonate (potassium salt)	Chlorpyrifosmethyl	Vinclozolin
Chlorhexidine Hydrochloride	Cyanofenphos	
1,2,5,6,9,10-Hexabromocyclododecane	Diazinon	
	Diazinon oxon	
	Dichlofenthion	
	Edifenphos	

(*continued on next page*)

Table 1 (*continued*)

Compounds		
Natural compounds and related chemicals (109)	Natural compounds (continued)	Medicines and cosmetic-related chemicals (58)
Natural compounds (72)	Melatonin	Medicines (30)
cis-Stilbene	Naringenin	Allyl-thiourea
trans-Stilbene	Naringin	Amiodarone
Azulene	Progesterone	5α-Androstane
Dibenzyl	Resveratrol	Benzophenone
Acridine	Retene	Benzoyl peroxide (BPO)
Flavone	9-cis-Retinoic Acid	Camphorquinone
Biochanin A	13-cis-Retinoic acid	Cinnarizine
Quercetin Dihydrate	all-trans-Retinal	Clofibrate
Genistein	all-trans-Retinoic acid	Clomiphene
17β-Estradiol	all-trans-Retinol	Cyproterone acetate
Zearalenone	3,5-Diiodo-L(+)-tyrosine dihydrate	Dexamethasone
Daidzein	T3 (3,5,3'-Triiodothyronine)	Dienestrol
β-Estradiol 3-Sulfate	T4 (3,3',5,5'-Tetraiodothyronine)	Diethylstilbestrol (DES)
β-Estradiol 3,17-Disulfate	3,3',5'-Triiodo-L-Thyronine	Dimethylaminoethyl methacrylic acid
β-Estradiol 17-(β-D-Glucuronide)	Vitamin A acetate	Dimetyl-p-toluidine
β-Estradiol 3-(β-D-Glucuronide)		Ethynylestradiol
Testosterone	Natural product-related chemicals (37)	Flutamide
Kaempferol	6,8-Dichlorochrysin	Hydroxypropionic Acid
Abietic Acid	6,8-Dichloroapigenin	4-Hydroxytamoxifen
Phloretin	3',8-Dichlorodaidzein	ICI 182780
Apigenin	3',5',8-Trichlorodaidzein	3-Iodo-L-tyrosine
4',5,7-Trihydroxyflavanone	6,8-Dichlorogenistein	Methyltrienolone
Coumestrol	6,8-Dichloronaringenin	Mibolerone
Genistin	6,8-Dichlorocatechin	5-Propyl-2-thiouracil
Daidzin	2-Chloroestrone (E1)	6-n-Propyl-2-thiouracil
17α-Estradiol	4-Chloroestrone (E1)	Spironolactone
Chrysin	2,4-Dichloroestrone (E1)	Tamoxifen
Luteolin	2,4,16,16-Tetrachloroestrone (E1)	3,3',5,5'-Tetraiodothyroacetic acid
Indole-3-Carbinol	10-Chloro-1,4-estradiene-3,17-dione	Thiamazole
Hesperetin	2-Chloro-17β-estradiol (E2)	3,3',5-Triiodothyroacetic acid
β-Sitosterol	4-Chloro-17β-estradiol (E2)	
Equol	2,4-Dichloro-17β-estradiol (E2)	Cosmetic-related chemicals (28)
Enterolactone	2-Chloroestriol (E3)	4-Aminobenzoic Acid
Formononetin	4-Chloroestriol (E3)	2-phenoxyethanol
β-Ecdysterone	2,4-Dichloroestriol (E3)	Ethyl 4-aminobenzoate
α-Ecdysterone	2-Chloro-17α-ethinylestradiol (EE2)	2-Ethylhexyl-4-p-dimethylamino-benzoate
Juvabione	4-Chloro-17α-ethinylestradiol (EE2)	2-Hydroxyethyl salicylate
Cyasterone	2,4-Dichloro-17α-ethinylestradiol (EE2)	4-t-Butylphenyl salicylate
Murisuterone A	4-Androstene-3,17-dione	4-Octylphenyl salicylate
Allylisothiocyanate	16,16-Dichloro-4-androstene-3,17-dione	Salicylic Acid 2-Ethylhexyl Ester
Catechin	1,4-Androstadiene-3,17-dione	2,4-Dihydroxy-benzophenone
Dehydroabietic acid	4,6-Cholestadien-3-one	2-Hydroxy-4-methoxy-benzophenone
5α-Dihydrotestosterone	2-Bromoestrone	2,2'-Dihydroxy-4-methoxy-benzophenone
Estriol	4-Bromoestrone	2,2',4,4'-Tetrahydroxybenzophenone
Estrone	2,4-Dibromoestrone	2,2'-Dihydroxy-4,4'-dimethoxy-benzophenone
Fisetin hydrate	2-Bromo-17β-estradiol	2-Hydroxy-4-n-octyloxy-benzophenone
Flavanone	4-Bromo-17β-estradiol	2-Hydroxy-4-methoxy-benzophenone-5-sulfonic acid
Galangin	2,4-Dibromo-17β-estradiol	4-t-Butyl-4'-methoxy-dibenzoylmethane
Harmol hydrochloride dihydrate	2-Bromoestriol	2-(2'-Hydroxy-5'-methylphenyl)-benzotriazole
Hesperidin	4-Bromoestriol	2-(2'-Hydroxy-5'-tert-butylphenyl)-benzotriazole
Hinokitiol	2,4-Dibromoestriol	2-(2'-Hydroxy-3',5'-di-tert-butylphenyl)-benzotriazole
Hydrocortisone	2-Bromo-17α-ethinylestradiol	2-(2'-Hydroxy-3',5'-di-tert-amylphenyl)-benzotriazole
6-Hydroxyflavanone	4-Bromo-17α-ethinylestradiol	2-(3',5'-Di-tert-butyl-2'-hydroxyphenyl)-5-chlorobenzotriazole
7-Hydroxyflavanone	2,4-Dibromo-17α-ethinylestradiol	2-(5-Chloro-2-benzotriazolyl)-6-tert-butyl-p-cresol
16α-Hydroxyestrone		3-(4-Methylbenzylidane)-camphor
11-Ketotestosterone		2-Ethylhexyl-4-Methoxycinnamate
		(±)-α-Tocopheryl Acetate
		Octamethylcyclotetrasiloxane
		Decamethylcyclopentasiloxane
		Dodecamethylcyclohexasiloxane

curve of the luminescence intensity of each compound was described, and two activity values were calculated from the power approximate expression. The EC × 10 was defined as the concentration of a test solution producing luminescence intensity 10 times that of the blank control, and the REC20 (20% relative effective concentration) was the concentration showing 20% of the activity of 10^{-8} M *all-trans* RA. Activity relative to RA was then calculated by dividing the REC20 of *all-trans* RA by that of a test compound. As there were no high volatile compounds in this study, loss of compounds by volatilization over an incubation period was not taken into consideration.

3. Results

3.1. Assay characteristics

The sensitivity and reproducibility of the RAR yeast assay were assessed using the endogenous ligand, *all-trans* RA. As a chemiluminescence method is used in which an

artificial substrate for β-galactosidase is added to sensitively detect transcriptional activation via the human RAR, the large amount of substrate did not allow luminescence intensity to reach a plateau, even at high concentrations of *all-trans* RA (Fig. 1). Therefore, the half-maximal effective concentration (EC_{50}) commonly used in this kind of *in vitro* assay was not reasonable to evaluate the agonistic ability of test chemicals in the present method. Instead of the EC_{50}, the EC × 10 of *all-trans* RA as defined above was 5.41 ± 1.73 nM (mean ± SD, 22 experiments, Table 2). Chemiluminescence intensity at 10^{-8} M *all-trans* RA was 21.2 ± 7.2 times that of the blank control, and then the REC20 was 2.19 ± 0.20 nM (Table 2).

3.2. Positive substances

Eighty-five of the 543 tested compounds, at their highest concentrations (10 μM), exhibited transcriptional agonistic activity via the human RARγ of at least 20% that of 10^{-8} M *all-trans* RA. Table 2 lists the positive substances in order of RARγ activation potency grouped into categories as for Table 1. The range of molecular weights was 164 (4-*n*-pentylphenol) to 444 (*trans*-nonachlor), and the range of total carbon number was 7 (chlorpyrifosmethyl) to 20 (*all-trans* retinol). Many of the tested organochlorine pesticides, styrene dimers, monoalkylphenols and parabens were found to be RARγ active.

3.3. Organochlorine pesticides

Sixteen of the tested 30 organochlorines had a positive effect on RARγ transfected yeast cells. γ-BHC was the most potent in this category and the activities of this compound and seven other organochlorines were over 0.1% (1/1000) of that of *all-trans* RA. The numbers of chlorine atoms in the active compounds were 6–9, while organochlorines out of this range had no effect on the RARγ.

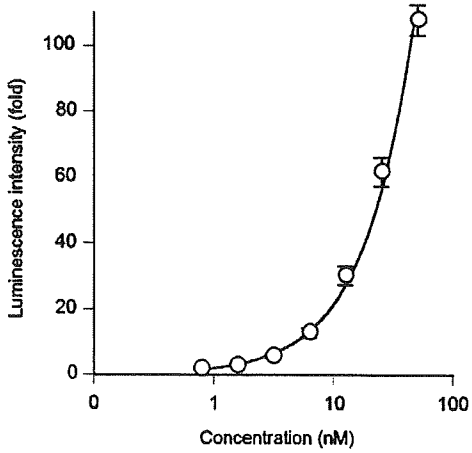

Fig. 1. Response of a yeast two-hybrid assay transfected with the human RARγ and the coactivator to the endogenous ligand, *all-trans* retinoic acid. Values are presented as n-fold induction over the vehicle control and as the mean ± SE of eight independent duplicate experiments.

3.4. Styrene dimers and trimers

All tested styrene dimers and a styrene dimer mixture of unspecified composition exhibited agonistic activity on the RARγ (Fig. 2), but styrene trimers had no effect. 1-Phenyltetralin and 1-methyl-3-phenylindan were particularly active styrene dimers with activities of over 0.6% of that of *all-trans* RA, while five other compounds had agonistic activities over 0.1%.

3.5. Monoalkylphenols

There were several highly active monoalkylphenols with 4-*n*-heptylphenol being the most potent compound tested in this study. All active monoalkylphenols had their alkyl chains *para* to the phenolic hydroxyl group, and the five most active compounds in this category had an alkyl group containing 6–9 carbons and their activities were over 0.4% of that of *all-trans* RA. The ranking of phenols having a linear alkyl group was heptyl (7 carbons) > hexyl (6) > octyl (8) > pentyl (5) > nonyl (9) > dodecyl (12) (Fig. 3). Branching of the alkyl group altered the potency of the phenols (Fig. 4). Comparison of REC20 values showed that an unspecified mixture of isomers of 4-nonylphenol was 4.7 times as active as 4-*n*-nonylphenol and that 4-tert-octylphenol was 2.2 times as active as 4-*n*-octylphenol. However, 4-tert-pentylphenol was 2.8-fold weaker than 4-*n*-pentylphenol. Moreover, six ring-chlorinated monoalkylphenols exhibited positive effects and had about the same or more potency than their unchlorinated analogs.

3.6. Parabens and other chemicals

Some alkyl *p*-hydroxybenzoates (parabens) with an alkyl group of 4–8 carbons were also positive to the RARγ. Of six positives, *n*-hexyl 4-hydroxybenzoate, *n*-pentyl 4-hydroxybenzoate and benzyl 4-hydroxybenzoate showed the highest agonistic activities with values over 0.1% that of *all-trans* RA. Phenols having a cyclic hydrocarbon side-chain *para* to the phenolic hydroxyl group (except 2-(1-adamantyl)-4-methylphenol), a hydroxyethyl ether of 4-nonylphenol and its chlorinated derivative were also positive to the RARγ, but with the exception of 4-(1-adamantyl)phenol, their activities were under 0.1% of that of *all-trans* RA. There were six active substances in the group that we have categorized as 'bisphenol-related compounds', namely, chlorinated bisphenol A and compounds found as impurities in industrial grade bisphenol A, but their activities, with the exception of 4-cumylphenol, were comparatively low. As shown in Table 2, there were also several active substances in the other categories, but most of these had a low potency for the RARγ. However, three diphenyl ethers, aclonifen, nitrofen and chlornitrofen, and the

Table 2
Responsiveness of a RARγ yeast assay to active compounds

Compounds	CAS No.	EC×10 (± SD, ×10^{-6} M)	REC20 (± SD, ×10^{-6} M)	Activity relative to RA (%)
all trans-Retinoic acid	302-79-4	0.00541 ± 0.00173	0.00219 ± 0.00020	100
Industrial chemicals (55)				
Aromatic hydrocarbons (4)				
2-Terphenyl	84-15-1	5.03 ± 2.43	1.77 ± 1.14	0.165
n-Octylbenzene	2189-60-8	20.09 ± 6.88	4.51 ± 2.52	0.065
1,3-Diphenylpropane	1081-75-0	8.68 ± 0.81	4.74 ± 1.10	0.062
Triphenylmethane	519-73-3	19.73 ± 4.76	5.34 ± 1.10	0.055
Bisphenols and related chemicals (6)				
2,2'-Dichlorobisphenol A	-	18.95 ± 7.05	6.15 ± 1.61	0.048
2,2',6-Trichlorobisphenol A	-	16.66 ± 5.30	7.85 ± 1.56	0.037
4-Cumylphenol	599-64-4	2.73 ± 0.58	1.68 ± 0.67	0.174
2-(4-Hydroxyphenyl)-2,4,4-trimethylchroman	-	6.53 ± 0.44	3.97 ± 1.33	0.074
2-(2-Hydroxyphenyl)-2,4,4-trimethylchroman	-	7.26 ± 0.96	4.57 ± 2.15	0.064
4-(4-Hydroxyphenyl)-2,2,4-trimethylchroman	472-41-3	6.98 ± 1.33	5.11 ± 2.00	0.057
Monoalkyl phenols and related chemicals (15)				
4-n-Heptylphenol	1987-50-4	0.49 ± 0.26	0.21 ± 0.11	1.363
4-t-Octylphenol	140-66-9	0.78 ± 0.41	0.29 ± 0.13	0.997
4-n-Hexylphenol	2446-69-7	0.69 ± 0.23	0.42 ± 0.13	0.695
4-Nonylphenol (mixed isomers)	84852-15-3	1.36 ± 0.70	0.62 ± 0.25	0.476
4-n-Octylphenol	1806-26-4	1.70 ± 0.56	0.66 ± 0.41	0.446
4-n-Pentylphenol	14938-35-3	3.43 ± 0.70	1.85 ± 0.44	0.159
4-n-Nonylphenol	104-40-5	4.61 ± 1.01	2.92 ± 1.10	0.100
4-Dodecylphenol (mixed isomers)	27193-86-8	5.45 ± 0.84	3.62 ± 0.72	0.081
4-t-Pentylphenol	80-46-6	9.92 ± 2.29	5.24 ± 1.33	0.056
2-Chloro-4-octylphenol	-	0.61 ± 0.37	0.23 ± 0.05	1.286
2,6-Dichloro-4-octylphenol	-	0.70 ± 0.16	0.28 ± 0.14	1.041
2-Chloro-4-nonylphenol	-	1.70 ± 0.96	0.69 ± 0.06	0.422
2,6-Dichloro-4-nonylphenol	-	2.77 ± 1.25	1.35 ± 0.41	0.217
2,6-Dichloro-4-butylphenol	-	4.64 ± 0.32	3.05 ± 0.96	0.096
2-Chloro-4-butylphenol	-	17.33 ± 4.12	7.94 ± 1.04	0.037
Parabens (6)				
n-Hexyl 4-hydroxybenzoate	1083-27-8	1.24 ± 0.26	0.75 ± 0.26	0.391
n-Amyl 4-hydroxybenzoate	6521-29-5	2.95 ± 0.26	1.92 ± 0.58	0.153
Benzyl 4-hydroxybenzoate	94-18-8	3.18 ± 0.55	2.26 ± 0.64	0.130
Isobutyl-4-hydroxybenzoate	4247-02-3	5.54 ± 0.93	4.08 ± 1.36	0.072
2-Ethylhexyl 4-Hydroxybenzoate	5153-25-3	5.58 ± 0.76	4.27 ± 0.90	0.069
Butyl-4-hydroxybenzoate	94-26-8	10.35 ± 2.66	6.37 ± 1.80	0.046
Phenols and related chemicals (7)				
4-(1-Adamantyl)phenol	29799-07-3	1.30 ± 0.80	0.54 ± 0.33	0.547
2-Chloro-4-nonylphenyl 2-hydroxyethyl ether	-	4.93 ± 1.33	3.21 ± 0.31	0.091
4-Cyclohexylphenol	1131-60-8	5.48 ± 1.00	3.23 ± 1.06	0.091
2-(1-Adamantyl)-4-methylphenol	41031-50-9	4.90 ± 0.68	3.82 ± 0.55	0.077
4-Nonylphenyl 2-hydroxyethyl ether	-	7.61 ± 2.34	4.35 ± 0.76	0.067
4-Benzylphenol	101-53-1	9.39 ± 3.55	4.74 ± 1.07	0.062
Hexestrol	5635-50-7	22.01 ± 3.51	7.00 ± 2.18	0.042

aromatic hydrocarbon 2-terphenyl showed agonistic activities over 0.1% of that of *all-trans* RA.

4. Discussion

The reactivity, reproducibility and dose-dependency of the RARγ yeast assay, using *all-trans* RA, as a standard, were satisfactory for assessing a wide range of chemicals as described here. The EC_{50} of *all-trans* RA in a reporter gene assay using RARγ-cotransfected HeLa cells and the IC_{50} in a competitive binding assay using RARγ-transfected COS-1 cells were reported to be 2.5 nM and 8 ± 1 nM, respectively (Bernard et al., 1992; Allenby et al., 1994). Although there is no simple comparison between these reports and our results, the responsivity of our assay system, which can be represented as EC × 10 or REC20 values, is within a similar range. Taking into account its simplicity and rapidity, application of this assay

Table 2 (*continued*)

Compounds	CAS No.	ECx10 (± SD, $\times 10^{-6}$ M)	REC20 (± SD, $\times 10^{-6}$ M)	Activity relative to RA (%)
all trans-Retinoic acid	302-79-4	0.00541 ± 0.00173	0.00219 ± 0.00020	100
Industrial chemicals (continued)				
Styrene dimers (14+1)				
1-Phenyltetralin	-	0.65 ± 0.02	0.25 ± 0.16	1.169
1-Methyl-3-phenylindan	-	1.22 ± 0.13	0.46 ± 0.28	0.632
trans-1,2-Diphenylcyclobutane	20071-09-4	3.37 ± 0.80	1.33 ± 0.75	0.220
1-Methyl-1-phenylindan	79034-12-1	4.77 ± 1.98	2.16 ± 0.81	0.135
cis-1,2-Diphenylcyclobutane	7694-30-6	5.43 ± 2.03	2.20 ± 1.12	0.133
2,4-Diphenyl-1-butene	16606-47-6	4.62 ± 0.69	2.32 ± 0.52	0.126
2,3-Diphenyl-1-butene	-	5.51 ± 2.81	2.40 ± 1.35	0.122
cis-1,4-Diphenyl-1-butene	-	6.22 ± 2.78	2.95 ± 1.38	0.099
trans-1,3-Diphenyl-1-butene	-	6.04 ± 1.91	2.99 ± 1.39	0.098
trans-1,3-Diphenylcyclobutane	-	7.09 ± 2.15	3.23 ± 1.39	0.091
1,4-Diphenyl-2-butene	-	8.29 ± 4.00	3.54 ± 1.62	0.083
cis-2,4-Diphenyl-2-butene	-	8.95 ± 2.77	3.89 ± 1.76	0.075
trans-1,4-Diphenyl-1-butene	-	8.62 ± 3.77	4.09 ± 1.84	0.072
trans-2,4-Diphenyl-2-butene	-	14.33 ± 4.49	6.83 ± 2.40	0.043
Polystyrene standard (mixed styrene dimer isomers)	-	7.54 ± 2.96	3.97 ± 0.77	0.074
Others (2)				
Octachlorostyrene	29082-74-4	21.93 ± 9.01	4.77 ± 3.47	0.061
Benzyl-2-naphthylether	613-62-7	21.98 ± 6.32	6.79 ± 0.37	0.043
Agrochemicals (22)				
Carbamate (1)				
Thiobencarb	28249-77-6	16.74 ± 1.64	5.48 ± 0.39	0.054
Diphenyl ethers (3)				
Aclonifen	74070-46-5	2.74 ± 0.62	1.33 ± 0.82	0.220
Nitrofen	1836-75-5	4.45 ± 1.31	2.18 ± 0.61	0.134
Chlornitrofen (CNP)	1836-77-7	7.77 ± 3.31	2.82 ± 1.22	0.104
Organochlorines (16)				
1,2,3,4,5,6-Hexachlorocyclohexane (γ-BHC)	58-89-9	0.89 ± 0.27	0.44 ± 0.14	0.668
Endrin	72-20-8	1.22 ± 0.79	0.85 ± 0.21	0.346
Heptachlor	76-44-8	2.09 ± 0.77	0.87 ± 0.37	0.336
Oxychlordane	27304-13-8	3.87 ± 0.99	1.90 ± 0.03	0.154
Chlordane	57-74-9	3.23 ± 1.89	1.93 ± 1.15	0.152
Toxaphene	8001-35-2	3.35 ± 1.64	2.59 ± 0.96	0.113
cis-Heptachlor epoxide	1024-57-3	3.46 ± 1.82	2.85 ± 0.60	0.103
cis-Chlordane	5103-71-9	5.63 ± 4.03	2.94 ± 1.33	0.100
trans-Chlordane	5103-74-2	7.15 ± 3.70	3.56 ± 1.80	0.082
β-Endosulfan	33213-65-9	9.06 ± 0.87	4.36 ± 2.71	0.067
Dieldrin	60-57-1	7.47 ± 4.60	4.70 ± 1.80	0.062
trans-Nonachlor	39765-80-5	7.74 ± 5.15	4.92 ± 0.30	0.060
Aldrin	309-00-2	8.88 ± 6.14	5.43 ± 0.91	0.054
β-Benzene hexachloride (β-BHC)	319-85-7	12.85 ± 3.15	5.69 ± 0.77	0.052
α-Endosulfan	959-98-8	8.02 ± 2.67	6.07 ± 2.40	0.048
trans-Heptachlor epoxide	1024-57-3 (trans)	8.49 ± 5.06	6.30 ± 1.58	0.047
Organophosphates (2)				
Cyanofenphos	13067-93-1	8.83 ± 1.51	3.42 ± 1.89	0.086
Chlorpyrifosmethyl	5598-13-0	13.81 ± 3.47	7.08 ± 2.11	0.041
Natural compounds and related chemicals (7)				
all-trans-Retinol	68-26-8	2.81 ± 0.17	1.67 ± 0.77	0.175
Flavanone	487-26-3	10.65 ± 1.14	4.23 ± 0.26	0.069
cis-Stilbene	645-49-8	10.16 ± 5.57	4.99 ± 2.58	0.059
Dibenzyl	103-29-7	17.95 ± 3.31	6.66 ± 2.10	0.044
4-Chloro-17β-estradiol	-	16.23 ± 3.77	4.35 ± 1.75	0.067
2,4-Dichloro-17β-estradiol	-	13.26 ± 1.52	4.79 ± 1.38	0.061
4-Bromo-17β-estradiol	-	12.49 ± 4.72	5.52 ± 3.91	0.053
Medicines and cosmetic-related chemicals (1)				
Cosmetic-related chemical (1)				
3-(4-Methylbenzylidane)-camphor	36861-47-9	15.98 ± 4.04	5.92 ± 1.85	0.050

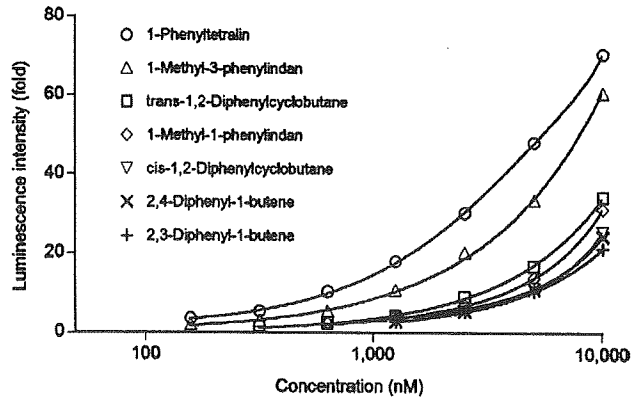

Fig. 2. Dose-response curves of styrene dimers in a RARγ yeast two-hybrid assay. Results are presented as the averages of a minimum of three duplicated experiments.

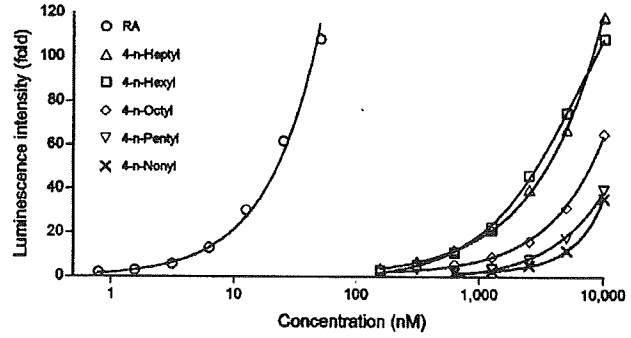

Fig. 3. Dose-response curves of monoalkylphenols having a linear alkyl group in a RARγ yeast two-hybrid assay. Results are presented as the averages of a minimum of three duplicated experiments.

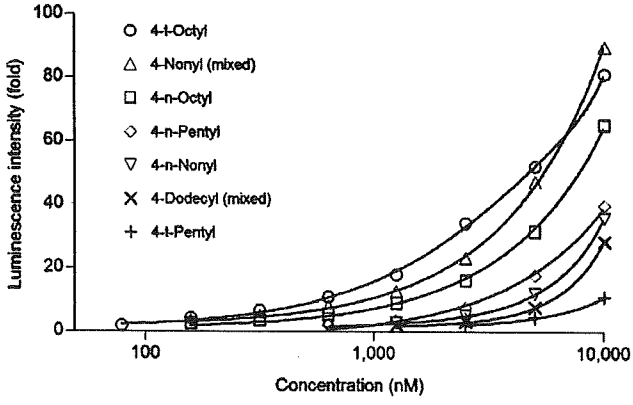

Fig. 4. Activity comparison of monoalkylphenols having a linear alkyl group with a branched group in a RARγ yeast two-hybrid assay. Results are presented as the averages of a minimum of three duplicated experiments.

using easily managed yeast cells to the toxicological evaluation of chemicals is appropriate and reasonable as a step in hazard identification with implications for mechanism of action. As RAs are known to undergo isomerization and oxidation when exposed to light and air (Bempong et al., 1995), some of the variability in the activity of *all-trans* RA can probably be attributed to the lability of the reagent to, in particular, photodegradation. However, the ready availability of an endogenous ligand for use in the assay more than compensates for this instability.

Many of the compounds active to the RARγ (organochlorines and styrene dimers were notable exceptions) were *para*-alkyl-substituted phenols. Phenols of this type are manufactured on a very large scale for many industrial purposes and have been reported to possess estrogenic activity, with the degree of activity depending on the length and branching of the alkyl substituent. Of the 4-*n*-alkylphenols, 4-*n*-nonylphenol had the highest binding affinity for the human ER (Tabira et al., 1999). 4-Alkylphenols having an alkyl group composed of 3–12 carbons, including branched groups (both secondary and tertiary), exhibited ER transactivation activity in a recombinant yeast assay (Routledge and Sumpter, 1997). There were some differences in the responsivities of the present RAR assay to alkyl and other phenols from those of the ER. The most potent activator of the RARγ was 4-*n*-heptylphenol and phenols with four or less carbons in their alkyl groups had no effect regardless of its position or branching. Alkylphenols having a branched alkyl group with many carbons, such as the mixed isomers of nonylphenol and tert-octylphenol, were more potent than analogs with a linear alkyl group, whereas of the pentylphenols with less carbon atoms in their alkyl groups, tert-pentylphenol is weaker than its analog with a linear alkyl group. This suggests that the overall length of a side-chain but not the actual number of carbons it contains may influence the potency of alkylphenols to the RARγ and that there may be an optimal length.

Ring-chlorinated alkylphenols had somewhat higher activity than their unchlorinated analogs, and bisphenol A, which had no positive effect on the RARγ, acquired agonistic activity by chlorination. This parallels observations in previous studies of estrogenicity where the estrogenic activities of chlorinated bisphenol A were stronger both *in vitro* and *in vivo* than those of the unchlorinated compound (Takemura et al., 2005; unpublished data, Shiraishi et al., 2000). Halogenation of chemicals might thus activate them or boost their actions on nuclear receptors. This is also indicated by observations in the present study that chlorination and bromination activated 17β-estradiol (E2) to the RARγ to a small extent. These findings suggest that not only in industrial manufacturing but in effluent processing, halogenation treatment does not reduce the unexpected activity of chemicals on nuclear receptors, but on the contrary might enhance the harmful effects.

We present here the first evidence that styrene dimers but not trimers have the ability to transactivate the RAR. The dimer 1-phenyltetralin was one of the most active chemicals revealed in this study. Furthermore, it was apparent that the fewer carbons linking the benzene rings of the dimers, the higher the agonistic activity (Figs. 2 and 5). Therefore, limited overall molecular length seems

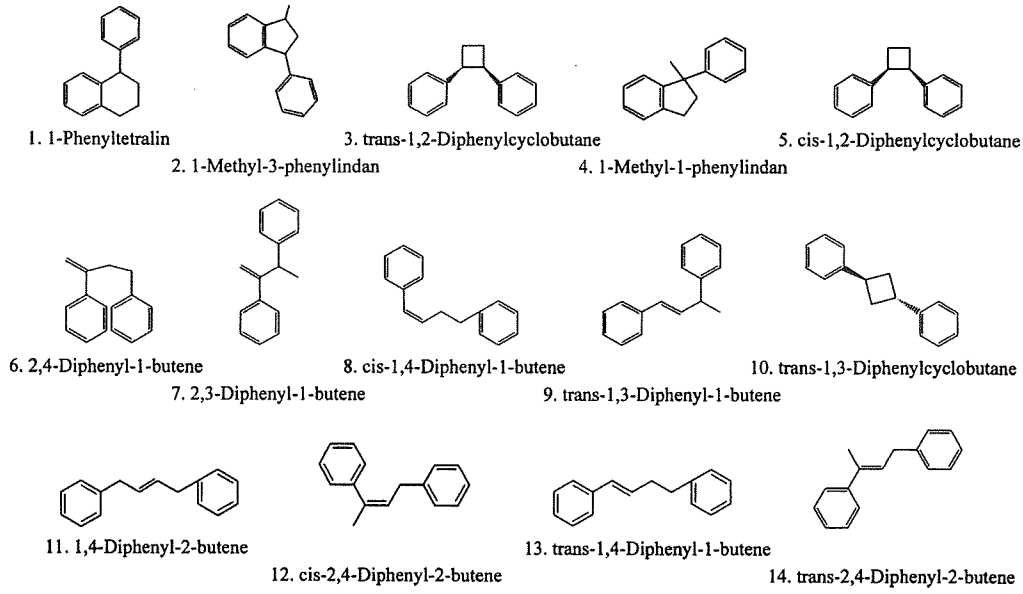

Fig. 5. Structural formulas of styrene dimmers.

to correlate with potency in styrene dimers. The lack of activity of styrene trimers may also arise from their length or size as the upper limit for the molecular weights of positive compounds (except halogenated compounds and organophosphates) was 286.5 (*all-trans* retinol), whereas the styrene trimers have molecular weights of 312. It is interesting that 2-terphenyl and 1,3-diphenylpropane have about the same activity as styrene dimers with similar structures (trans-1,2-diphenylcyclobutane and trans-2,4-diphenyl-2-butene, respectively). The binding affinity of these chemicals for the RAR may depend on molecular length, like alkylphenols as discussed above. Styrene oligomers also have binding affinity for the human ER (Ohyama et al., 2001; Kitamura et al., 2003). Importantly, it has been reported that styrene trimers exhibit *in vivo* disruption of endocrine systems and that embryonic exposure obstructs genital organ development and disrupts the endocrine function of male rat offspring (Ohyama et al., 2007). Polystyrene resins contain substantial amounts of styrene dimers and trimers, and extraction tests with polystyrene food containers have shown that these compounds leak into the food, water and oil with which they are in direct contact (Kawamura et al., 1998a,b,c). Because all styrene dimers tested in this study had a positive effect on the RARγ and selective ligands for the RAR subtypes are teratogenic in the developing embryo, the developmental toxicity of styrene oligomers via the RAR as well as the ER should be investigated.

Organochlorine pesticides were previously reported to transactivate RARβ and γ, but not RARα in human RAR reporter cell lines (Lemaire et al., 2005). The tested five organochlorines had dose-dependent effects on the RARγ and the order of potency was endrin > dieldrin > aldrin > chlordane > endosulfan, although even the activity of endrin was only approximately 1/12000 of that of the standard RAR agonist, (*E*)-4-[2-(5,6,7,8-tetrahydro-5,5,8,8-tetramethyl-2-naphthylenyl)-1-propenyl] benzoic acid. Our results indicated that many organochlorines, including those five compounds examined, also have the potential to activate the RARγ. The present yeast assay detected the activities of these compounds at lower concentrations than the reported cell line. In addition, our assay results indicated that binding affinity for the RAR partially depends on the number of chlorine atoms in the molecule and that there seems to be an optimal range of their chlorine number. Many studies have shown that a number of pesticides, including organochlorines, possess estrogenic activity (Hodges et al., 2000; Kojima et al., 2004), but their potencies for the ER do not correspond with those for the RAR. For example, the ranking of the activities of organochlorines for the ERs in Chinese hamster ovary cells are *o,p'*-DDT (4.5×10^{-8} M, test compound concentration showing 20% of the agonistic activity of 10^{-10} M 17β-estradiol) > β-BHC (3.5×10^{-7} M) > methoxychlor (5.6×10^{-7} M) for the ERα, and β-BHC (1.1×10^{-7} M) > *o,p'*-DDT (1.2×10^{-7} M) > δ-BHC (1.1×10^{-6} M) for the ERβ (Kojima et al., 2004), whereas none of these compounds showed a significant effect on the RARγ in our assay system. Because persistent and/or harmful pesticides such as organochlorines are now prohibited in developed countries, but still used in developing regions, detailed investigations of their toxicity via nuclear receptors, as well as a global restriction on their use, are required.

The present study illustrated that a number of compounds possessed unexpected transcriptional activation effects on the human RARγ in a yeast two-hybrid system, as we have already shown for the ERs and TRs (Shiraishi et al., 2003; Arulmozhiraja et al., 2005; Morohoshi et al., 2005). It is common for xenobiotics to have low affinity for nuclear receptors relative to the natural ligands, as we

reported here. However, there are a number of examples (principally from the ER, which is better studied than the RAR) where man-made compounds produce adverse effects in living organisms via nuclear receptors. Agonistic ligands for nuclear receptors such as the RARs and ERs have been confirmed the ability to experimentally induce developmental abnormalities (Elmazar et al., 1996, 2001; Kamata et al., 2006), and there are medically or environmentally documented cases of their teratogenicities (Lammer et al., 1985; Fry, 1995; Sumpter, 1998). For example, in previous studies, the REC20 of 2,2′,4′6′-tetrachlorobiphenyl-4-ol, one of monohydroxylated polychlorinated biphenyls, was 24 nM in our human ERα yeast assay, and its activity relative to E2 was 1.7% (Arulmozhiraja et al., 2005). *In ovo* exposure to this compound at a dose of 100 ng/g egg or more caused shortening of the oviduct in female Japanese quails and a dose of 500 ng/g or more caused a reduction testis weight in males after sexual maturation (Kamata et al., 2006). This dose range in ovo was approximately 100 times higher than a positive control, diethylstilbestrol, producing *in vitro* effect equivalent to E2. Recently, the existence of environmental pollutants having binding affinity for less researched but important nuclear receptors, such as the retinoid X receptors (RXR) and peroxisome proliferator-activated receptors (PPAR), and consequential disorders in organisms has been reported (Nishikawa et al., 2004; Abbott et al., 2007; Takacs and Abbott, 2007). Both tributyltin and triphenyltin used in antifouling paints exhibited agonistic activity in yeast assays transfected with the human RXR (α, β or γ) at a concentration of 10 nM or more, and this concentration was somewhat lower than that of 9-*cis* RA, the natural ligand of RXR (Nishikawa et al., 2004). One injection of 1 μg triphenyltin/g wet weight induced the differentiation and growth of male genital tracts in female gastropods, *Thais clavigera*, which was also stronger than 9-*cis* RA (Nishikawa et al., 2004). Thus, these reports are typical cases that *in vitro* affinity of chemicals for nuclear receptors is well correlated with their *in vivo* potential, and therefore, measurement of the relative activity of chemicals using *in vitro* assays seems to be valuable to estimate the *in vivo* effects of them.

There is great concern that substances released into the environment and/or used in everyday life may influence human and wildlife health. Detection of chemicals with an affinity for the various receptors is an important step in hazard identification. This data can be used to direct and prioritize additional research and *in vivo* studies on chemicals that bind nuclear receptors for possible receptor-mediated toxicity and endocrine disrupting activity. As described here, yeast assay systems including a RAR assay are useful for high-throughput screening of substances active to nuclear receptors.

5. Conflict of interest

There are no conflicts of interests involved in this study.

Acknowledgement

The authors thank Ms. Miho Yamasaki for skilful technical assistance.

References

Abbott, B.D., Wolf, C.J., Schmid, J.E., Das, K.P., Zehr, R.D., Helfant, L., Nakayama, S., Lindstrom, A.B., Strynar, M.J., Lau, C.S., 2007. Perfluorooctanoic acid (PFOA)-induced developmental toxicity in the mouse is dependent on expression of peroxisome proliferator activated receptor-alpha. Toxicological Sciences 98, 571–581.

Allenby, G., Janocha, R., Kazmer, S., Speck, J., Grippo, J.F., Levin, A.A., 1994. Binding of 9-*cis*-retinoic acid and *all-trans*-retinoic acid to retinoic acid receptors α, β, and γ. Retinoic acid receptor gamma binds *all-trans*-retinoic acid preferentially over 9-*cis*-retinoic acid. Journal of Biological Chemistry 269, 16689–16695.

Arulmozhiraja, S., Shiraishi, F., Okumura, T., Iida, M., Takigami, H., Edmonds, J.S., Morita, M., 2005. Structural requirements for the interaction of 91 hydroxylated polychlorinated biphenyls with estrogen and thyroid hormone receptors. Toxicological Sciences 84, 49–62.

Bempong, D.K., Honigberg, I.L., Meltzer, N.M., 1995. Normal phase LC–MS determination of retinoic acid degradation products. Journal of Pharmaceutical and Biomedical Analysis 13, 285–291.

Bernard, B.A., Bernardon, J.M., Delescluse, C., Martin, B., Lenoir, M.C., Maignan, J., Charpentier, B., Pilgrim, W.R., Reichert, U., Shroot, B., 1992. Identification of synthetic retinoids with selectivity for human nuclear retinoic acid receptor gamma. Biochemistry and Biophysical Research Communications 186, 977–983.

Elmazar, M.M., Reichert, U., Shroot, B., Nau, H., 1996. Pattern of retinoid-induced teratogenic effects: possible relationship with relative selectivity for nuclear retinoid receptors RAR alpha, RAR beta, and RAR gamma. Teratology 53, 158–167.

Elmazar, M.M., Ruhl, R., Nau, H., 2001. Synergistic teratogenic effects induced by retinoids in mice by coadministration of a RARα- or RARγ-selective agonist with a RXR-selective agonist. Toxicology and Applied Pharmacology 170, 2–9.

Fry, D.M., 1995. Reproductive effects in birds exposed to pesticides and industrial chemicals. Environmental Health Perspectives 103 (Suppl. 7), 165–171.

Hodges, L.C., Bergerson, J.S., Hunter, D.S., Walker, C.L., 2000. Estrogenic effects of organochlorine pesticides on uterine leiomyoma cells *in vitro*. Toxicological Sciences 54, 355–364.

Kamata, R., Takahashi, S., Shimizu, A., Morita, M., Shiraishi, F., 2006. *In ovo* exposure quail assay for risk assessment of endocrine disrupting chemicals. Archives of Toxicology 80, 857–867.

Kawamura, M., Nishi, K., Maehara, T., Yamada, T., 1998a. Migration of styrene dimers and trimers from polystyrene containers into instant foods. Journal of the Food Hygiene Society of Japan 39, 390–398.

Kawamura, M., Sugimoto, N., Takeda, Y., Yamada, T., 1998b. Identification of unknown substances in food contact polystyrene. Journal of the Food Hygiene Society of Japan 39, 110–119.

Kawamura, Y., Kawamura, M., Takeda, Y., Yamada, T., 1998c. Determination of styrene dimers and trimers in food contact polystyrene. Journal of the Food Hygiene Society of Japan 39, 199–205.

Kitamura, S., Ohmegi, M., Sanoh, S., Sugihara, K., Yoshihara, S., Fujimoto, N., Ohta, S., 2003. Estrogenic activity of styrene oligomers after metabolic activation by rat liver microsomes. Environmental Health Perspectives 111, 329–334.

Kojima, H., Katsura, E., Takeuchi, S., Niiyama, K., Kobayashi, K., 2004. Screening for estrogen and androgen receptor activities in 200 pesticides by *in vitro* reporter gene assays using Chinese hamster ovary cells. Environmental Health Perspectives 112, 524–531.

Lammer, E.J., Chen, D.T., Hoar, R.M., Agnish, N.D., Benke, P.J., Braun, J.T., Curry, C.J., Fernhoff, P.M., Grix Jr., A.W., Lott, I.T., et al.,

1985. Retinoic acid embryopathy. New England Journal of Medicine 313, 837–841.

Lemaire, G., Balaguer, P., Michel, S., Rahmani, R., 2005. Activation of retinoic acid receptor-dependent transcription by organochlorine pesticides. Toxicology Applied Pharmacology 202, 38–49.

Mispagel, C., Shiraishi, F., Allinson, M., Allinson, G., 2005. Estrogenic activity of treated municipal effluent from seven sewage treatment plants in Victoria, Australia. Bulletin of Environmental Contamination and Toxicology 74, 853–856.

Morohoshi, K., Yamamoto, H., Kamata, R., Shiraishi, F., Koda, T., Morita, M., 2005. Estrogenic activity of 37 components of commercial sunscreen lotions evaluated by *in vitro* assays. Toxicology in Vitro 19, 457–469.

Nishikawa, J., Mamiya, S., Kanayama, T., Nishikawa, T., Shiraishi, F., Horiguchi, T., 2004. Involvement of the retinoid X receptor in the development of imposex caused by organotins in gastropods. Environmental Science and Technology 38, 6271–6276.

Nishikawa, J., Saito, K., Goto, J., Dakeyama, F., Matsuo, M., Nishihara, T., 1999. New screening methods for chemicals with hormonal activities using interaction of nuclear hormone receptor with coactivator. Toxicology and Applied Pharmacology 154, 76–83.

Ohyama, K., Satoh, K., Sakamoto, Y., Ogata, A., Nagai, F., 2007. Effects of prenatal exposure to styrene trimers on genital organs and hormones in male rats. Experimental Biology and Medicine (Maywood) 232, 301–308.

Ohyama, K.I., Nagai, F., Tsuchiya, Y., 2001. Certain styrene oligomers have proliferative activity on MCF-7 human breast tumor cells and binding affinity for human estrogen receptor. Environmental Health Perspectives 109, 699–703.

Routledge, E.J., Sumpter, J.P., 1997. Structural features of alkylphenolic chemicals associated with estrogenic activity. Journal of Biological Chemistry 272, 3280–3288.

Shiraishi, F., Okumura, T., Nomachi, M., Serizawa, S., Nishikawa, J., Edmonds, J.S., Shiraishi, H., Morita, M., 2003. Estrogenic and thyroid hormone activity of a series of hydroxy-polychlorinated biphenyls. Chemosphere 52, 33–42.

Shiraishi, F., Shiraishi, H., Nishikawa, J., Nishihara, T., Morita, M., 2000. Development of a simple operational estrogenicity assay system using the yeast two-hybrid system. Journal of Environmental Chemistry 10, 57–64.

Sumpter, J.P., 1998. Xenoendorine disrupters-environmental impacts. Toxicology Letters 102–103, 337–342.

Tabira, Y., Nakai, M., Asai, D., Yakabe, Y., Tahara, Y., Shinmyozu, T., Noguchi, M., Takatsuki, M., Shimohigashi, Y., 1999. Structural requirements of *para*-alkylphenols to bind to estrogen receptor. European Journal of Biochemistry 262, 240–245.

Takacs, M.L., Abbott, B.D., 2007. Activation of mouse and human peroxisome proliferator-activated receptor (α, β/δ, γ) by perfluorooctanoic acid and perfluorooctane sulfonate. Toxicological Sciences 95, 108–117.

Takemura, H., Ma, J., Sayama, K., Terao, Y., Zhu, B.T., Shimoi, K., 2005. *In vitro* and *in vivo* estrogenic activity of chlorinated derivatives of bisphenol A. Toxicology 207, 215–221.

Zile, M.H., 1998. Vitamin A and embryonic development: an overview. Journal of Nutrition 128, 455S–458S.

Zile, M.H., 2001. Function of vitamin A in vertebrate embryonic development. Journal of Nutrition 131, 705–708.